# PERFORMANCE PREDICTION MODELLING AND THERMAL ANALYSIS OF HEAT RESISTANT CLOTHING

**A Thesis Submitted**
**In Fulfillment of the Requirements**
**for the Degree of**

## DOCTOR OF PHILOSOPHY

*In*

**Mechanical Engineering**

**By**

**ASHUTOSH KUMAR RAI**

**(2K15/PhD/ME/09)**

**Under the Supervision of**

***Prof. B.B. Arora***
**Professor**
**Department of Mechanical Engineering**
**Delhi Technological University**


**DELHI TECHNOLOGICAL UNIVERSITY**
**(Formerly Delhi College of Engineering)**
**Shahbad Daulatpur, Main Bawana Road, Delhi-110042. India**

**December, 2024**

**DELHI TECHNOLOGICAL UNIVERSITY**
**(Formerly Delhi College of Engineering)**
**Shahbad Daulatpur, Main Bawana Road, Delhi-110042. India**

## DECLARATION

I, Ashutosh Kumar Rai, (2K15/PhD/ME/09) hereby declare that the thesis entitled ***"Performance Prediction Modelling and Thermal Analysis of Heat Resistant Clothing"*** submitted by me, is an original and authentic work carried out by me under the supervision of **Prof. B.B. Arora,** Professor, Department of Mechanical Engineering, Delhi Technological University, Delhi for the award of the degree of ***Doctor of Philosophy*** in ***Mechanical Engineering***. I further declare that the work reported in this thesis has not been submitted and will not be submitted, either in part or in full, for the award of any other degree or diploma in this Institute or any other Institute or University.

Place: Delhi

Date: 05th December 2024

**ASHUTOSH KUMAR RAI**
(2K15/PhD/ME/09)
PhD Scholar
Department of Mechanical Engineering
Delhi Technological University.

**DELHI TECHNOLOGICAL UNIVERSITY**
**(Formerly Delhi College of Engineering)**
**Shahbad Daulatpur, Main Bawana Road, Delhi-110042. India**

# CERTIFICATE

Certified that **Ashutosh Kumar Rai** (2K15/PhD/ME/09) has carried out his research work presented in this thesis entitled **"Performance Prediction Modelling and Thermal Analysis of Heat Resistant Clothing"** for the award of degree of **Doctor of Philosophy** from Delhi Technological University New Delhi, under my supervision. The thesis embodies results of original work, and studies are carried out by the student himself and the contents of the thesis do not form the basis for the award of any other degree to the candidate or to anybody else from this or any other University/Institution.

**(Prof. B. B. Arora)**
Professor
Department of Mechanical Engineering
Delhi Technological University
Delhi 110042

Date: 5th December 2024

# ACKNOWLEDGEMENT

It is a great pleasure to have the opportunity to extend my heartiest felt gratitude to everybody who helped me throughout the course.

It is distinct pleasure to express my deep sense of gratitude and indebtedness to my learned supervisor Prof. B.B. Arora, Head, Department of Mechanical, Production, Industrial, and Automobile Engineering, Delhi Technological University, Delhi for his invaluable guidance, encouragement, and patient review. Their continuous inspiration only has enabled me to complete this research work.

I would like to express my gratitude to Prof. Prateek Sharma, Vice chancellor, Delhi Technological University, Delhi for providing this opportunity to carry out my work in this prestigious institute.

I wish to record my thanks and gratitude to all External and Internal SRC experts, Prof. R.P. Gakkhar (IIT Roorkee), Prof. J.A Usmani (Jamia Millia Islamia, New Delhi), Prof. Vipin Kumar (DTU, Delhi) and Prof. S. Maji (DTU, Delhi) for their valuable guidance, critical and constructive discussion during this work

I am thankful to my family members, friends and classmates for their unconditional support and motivation.

December 2024 **Ashutosh Kumar Rai**

# ABSTRACT

Heat resistant clothing is the primary component for the effective and safe performance of firefighting operations. Firemen who actually go into the fire to rescue people are themselves prone to fire burns. Hence, heat resistant clothing is essential for safety of fire fighters and effective rescue operations. Heat resistant clothing prevents heat from the fire reaching the human body and saves the fireman from being exposed directly to the fire. This is achieved by preventing heat conduction and by reflecting most of the heat flux incident on the clothing.

However, if the heat resistant clothing fails when the fireman is going through the flames or near it for rescue operations, then it will pose a serious threat to the life of the fireman. The human body can tolerate temperature roughly around 50-55$^0$C whereas the temperature of the fire is 20 times this limit. So if a fire suit fails in actual fire conditions, then it will definitely cause heavy personal injury to the fireman using the clothing and will further hamper the rescue operations. Hence it is extremely crucial to stringently test the heat resistant clothing before rendering it safe within the prescribed limits for real life fire scenarios.

Fire fighters' heat resistant suit is designed to offer the wearer with a limited amount of safety from burn injury if suddenly exposed to an intense short duration flash fire or short time exposure to a flashover condition. This level of protection has been made possible through the development of new heat resistant fabrics and insulating materials. Though there has been a rapid development in the fire protective materials, but the test and evaluation procedures for complete fire protective ensembles still lack behind.

So far humans have been used to test the clothing. A person actually wears the clothing and walks into a manmade fire. If he feels heat then he makes some signal and the fire is immediately extinguished by firemen. This is a very crude and inaccurate method for testing the clothing as the actual heat conduction of the clothing cannot be accurately deduced. Moreover, the heat tolerance varies from person to person and also if the heat resistant clothing is not suitable, it will immediately cause personal injury to the person testing the clothing.

This necessitates alternative methods for testing heat resistant clothing which will not only eliminate humans from actually going into the fire for testing the clothing but also gives more accurate and reproducible test results. This can be achieved by design and development of Fire Suit Evaluation Facility in which a human dummy is used for testing. The instrumented manikin, fitted with sensors, is exposed to a known heat flux. The data from the instrumented manikin is used for analysing the performance of the suit. The data is further utilized for burn injury prediction. This is a completely automated state of the art facility and one of its kinds in the country. This alternative method envisaged for the testing of heat resistant clothing is as per internationally accepted ASTM F1930 standard.

In addition, Modelling & Simulation is undertaken to model different types of heat resistant Ensembles and to predict their performance for different fire environments. The simulated model is validated against the experimental results. The development of modelling and simulation capability enabled more accurate performance prediction of futuristic materials & fire protective ensembles. This method further aid in reduction of design & development time required for the same.

# CONTENTS

# LIST OF TABLES

# LIST OF FIGURES

# List of Symbols and Abbreviations

**Notations**

| | |
|---|---|
| $A$ | area ($m^2$) |
| $C_p$ | specific heat (kJ $Kg^{-1}K^{-1}$) |
| $h$ | enthalpy (kJ $kg^{-1}$) |
| $H$ | water head (m) |
| $h_c$ | heat transfer coefficient (kW $m^{-2}K^{-1}$) |
| $h_M$ | mass transfer coefficient (kW $m^{-2}s^{-1}$) |
| $L_e$ | Lewis number (-) |
| $L_w$ | Latent heat of water (kJ $kg^{-1}$) |
| $\dot{m}$ | mass flow rate ($kgs^{-1}$) |
| $P$ | pressure (kPa) |
| $\dot{P}$ | Power (kW) |
| $\dot{q}_l$ | latent heat transfer rate (kW) |
| $\dot{q}_s$ | sensible heat transfer rate (kW) |
| $RH$ | relative humidity (%) |
| $s$ | entropy ($kJ.kg^{-1}K^{-1}$) |
| $T$ | temperature (°C) |
| $U$ | overall heat transfer ($kW.m^{-2}K^{-1}$) |
| $w$ | specific work (kJ $kg^{-1}$) |
| $W$ | power input (kW) |

**Greek symbols**

| | |
|---|---|
| $\delta$ | thickness (m) |
| $\nu$ | specific volume ($m^3$ $kg^{-1}$) |
| $\rho$ | density (kg $m^{-3}$) |
| $\varphi$ | maintenance factor (-) |
| $\omega$ | specific humidity (kg/kg of dry air) |
| $\Delta$ | difference |
| $\Psi$ | exergy ratio (-) |

**Subscripts**

| | |
|---|---|
| a | air |
| $EL$ | unit electricity (kWh) |
| ENV | environmental |
| i | inlet, inside |
| LM | log mean |
| o | outlet, outdoor |
| R | room |
| s | saturation |
| sh | superheat |
| t | total |
| w | water |

# CHAPTER 1

# INTRODUCTION

This chapter provides the need of Fire Fighting Ensemble/ heat resistant clothing. Different fabric layers, their properties and skin burns has been described. Testing methods for fabrics and complete body fire suits has been elaborated. At the end, the organisation of this thesis is presented.

## 1.1 BACKGROUND

Predicting the performance and conducting thermal analysis of heat-resistant clothing are crucial aspects in ensuring the safety and effectiveness of such apparel, especially in industries like firefighting, foundries, and aerospace.

Firefighters work in harsh conditions, including high temperatures and other potentially fatal situations. Fire suit is the only protection from the high heat flux exposures. It will be able to protect the human skin by providing a protective layer between skin and heat. Our firefighters may have severe burn or damage to health while working to IDLH environment in the absence of safety gears. Fire suit is one the most important safety gear for the firefighters.

Materials like aramid fibers (e.g., Nomex), para-aramid fibers (e.g., Kevlar), and meta-aramid fibers (e.g., Conex) are common due to their high strength and heat resistance. As per National Fire Protection Association (NFPA) 1971 fire suits (including fabric, zip and stitching) should be flame retardant and the properties of the materials should not be affected due to washing and daily use.

National Fire Protection Association (NFPA) prepare standards for the specifications of firefighting equipment and protective gears. The standard provide clarification for the testing procedure and certification of firefighting protective gears. These gears are helmet, coat, pant, gloves and shoes.

ASTM F1930 is a standard test method used for the evaluation of flame resistant clothing by the use of manikin instrumented with several heat flux sensors as per the standard.

## 1.2 FIREFIGHTING SUITS

A firefighting suit is specialized personal protective equipment (PPE) worn by firefighters to protect them from hazards they face while combating fire. Components of firefighting suits are Helmet, Hood, Jacket, Pants, Gloves, Boots and Self-Contained Breathing Apparatus (SCBA). There are two types of firefighting suits as per NFPA 1971.

(a) Structural Firefighting Suit

(b) Proximity Suit

These suits are further classified into Entry Suit and Approach Suit.

Following are the different types of Fire suits.

**1.2.1 Approach Suits:** Approach suits are used to work in the high temperature areas, e.g. smelting plants, steel mills and similar plants. It provides $200^{O}$ F ($93^{O}$ C) of maximum ambient heat protection.

**Fig. 1.1** Structural Fire suit

**1.2.2 Proximity Suits:** Aircraft rescue and fire-fighting (AR-FF) operations uses the proximity suits. Entry into the heated kiln is also needed this suit. Maximum ambient heat protection is about $500^{O}$ F ($260^{O}$ C).

**Fig. 1.2** Proximity Fire suit

**1.2.3 Entry Suits:** When entering extremely hot environments or circumstances where complete flame engulfment is required, entry suits are utilized.

**1.2.4 Wildland Suits:** Wildland Firefighter Suits allow firemen to work for extended periods of time in close proximity to heat and flames while providing protection while battling fires in places like forests and heath regions. Firefighters who wear wildland suits get heat exhaustion from intense physical work in hot, dry weather. Applicable standard for wildland suits are NFPA 1977 & ISO 16073.

**Fig. 1.3** Wildland Fire suit

## 1.3 FABRIC LAYERS/ COMPONENTS

Multilayer fire suits are usually comprised of three main layers. The outermost layer, middle layer and inner layer. The majority of physical damage and thermal insults are directed towards the outer layer. The moisture barrier, which shields the thermal liner, is the middle layer. The primary barrier against burns for firefighters is the thermal liner, which comes into direct contact with their skin.

**1.3.1 Outer Layer**: Fire suit's outermost layer serves as its first line of defence. This layer's materials are made to withstand direct flame and heat exposure without deteriorating or burning. Nomex, Kevlar, Basofil, Mellenia and PBI are examples of materials used in outer shell design. The significant wear and tear that comes with

combating fires requires these materials to be strong. Although outside shells are typically finished with water resistance, the inner layer offers the majority of moisture protection.

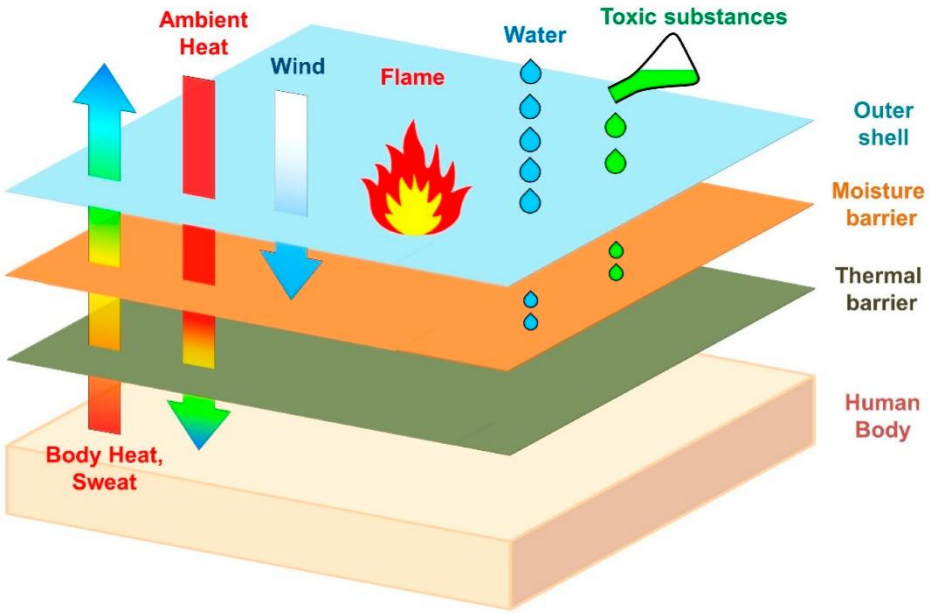


**Fig. 1.4** Layers of Fire suit

**1.3.2 Moisture Barriers:** Middle layer of the fire suit is the most important fabric in the construction. This layer's primary goal is to keep the thermal liner dry so that highly conductive moisture won't impair the liner's insulating properties. Because the materials that make up this layer are breathable and waterproof, heat and moisture may escape but cannot enter. Total heat loss (THL), or the amount of energy permitted to pass through the moisture barrier, is a measure of the barrier's effectiveness. In the case of structural firefighting suits this layer is made of PU coating over e-PTFE and further laminated over Meta-aramid. In the case of proximity suit moisture barrier is made by the Neoprene coating over glass fabric which is non-breathable.

**1.3.3 Thermal Liners:** This layer needs to be capable of managing moisture, offering comfort on the skin, and providing thermal protection. Current requirements mandate that thermal liners be either permanently stitched in or button removable. The thermal liner protects the user from radiation, convection, and conduction heat, making up around 75% of the total thermal protection offered by the three layers.

The face cloth and non-woven batting are the two primary parts of the thermal liner. The potion that comes into touch with the user's skin is the face cloth, which is usually made of fire-retardant cotton or a woven inner material like Nomex. This material is attached to a non-woven thermal insulator by quilting or lamination. The batting's air gaps and the insulator's fibers give the necessary thermal resistance. Blends of Nomex and Kevlar (WFR) are used to make the majority of thermal battings.

**1.3.4 Inner Liners:** This layer is made of FR Cotton (50% FR Viscose + 50% meta aramid)

Depending upon the fire scenario, there exist primarily two main types of firefighting operations viz. structural firefighting and proximity firefighting operations. Different type of firefighting suits are required to deal with these fires. Structural firefighting is a generalised firefighting operation and includes activities of rescue, fire suppression, and property conservation in buildings, enclosed structures, aircraft interiors, vehicles, vessels, or like properties that are involved in a fire. The clothing for structural firefighting includes a non-reflective outer layer, a breathable moisture barrier and a thermal insulation layer.

Proximity firefighting on the other hand, is a specialized firefighting operation, which includes activities of rescue, fire suppression, and property conservation at areas involving fires producing high levels of radiant heat as well as conductive and convective heat. Specialized thermal protection is necessary for persons involved in such operations due to the scope of these operations and the close distance to the fire at which these operations are conducted, although direct entry into

flame is not made. Examples of proximity firefighting include firefighting activities involving aircraft and bulk flammable fuels. These suits are also commonly used by firefighters in the defence services.

This clothing is an ensemble of several layers; each having its own specific role to play as per its placement in the configuration. A representative assembly is presented in Fig 1.5. The present generation proximity clothing is an ensemble of various layers, which conforms to international standards like EN 1486 or NFPA 1971. Due to the high levels of radiant heat involved, the outer shell of proximity fire protective suits is made up of aluminized reflective layer. Aluminized protective clothing offers a means of providing protection to fire fighters because of its high percentage of reflectivity (>90%) to radiant heat. Next in the ensemble is a durable, waterproof moisture barrier fabric, which prevents water ingress to the underlying insulating layer. Underneath, a thermal barrier layer is placed, which provides requisite level of thermal insulation to the wearer.

Thus the first layer of defence in a fire proximity clothing ensemble is a reflective outer layer, the role of which is to reflect back 90-95% of the radiant heat. This layer is generally prepared by laminating a metalised film on a suitable base fabric, most commonly being a woven glass textile. For the said application, this layer has to pass several tests, the most stringent being a radiant protective performance (RPP) test where in an abraded sample should be able to reflect the radiant component of heat. During the abrasion cycle, a significant fraction of this metalized film is abraded, and therefore the requisite level of radiant protection is difficult to achieve. Another important test, where failure generally occurs is the wet flex testing. In this case, the failure in the aluminised glass fabric occurs due to cracking of external aluminium layer on PET and also due to delamination of inner aluminized surface of PET and glass fabric. This essentially implies that there should be excellent adhesion of the deposited aluminium metal with the PET film as well as that of the aluminised PET with the base fabric. The requirements of the outermost layer as per the mentioned standards is presented in Table 1.1.

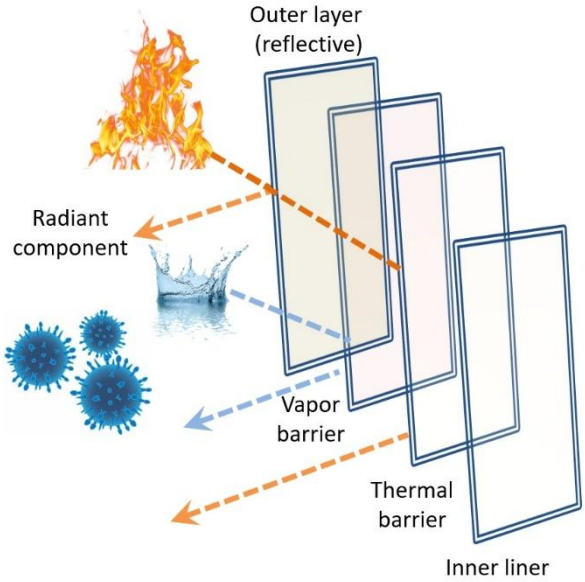


**Fig 1.5** A schematic representation of the multilayer ensemble of fire proximity suit

**Table 1.1** Comparison of selected standard requirement for fire proximity suit (w.r.t outermost layer)

| **Category** | **Standard** | **Parameter** | **Requirements** | **Standard test method** |
|---|---|---|---|---|
| Heat transfer (radiant exposure) | NFPA 1971 | RPP (Radiant protective performance) Radiant heat: 84kW/$m^2$<br><br>(Test to be performed after 300 abrasion cycle as per ASTM D4157) | Intersection time of not less than 20 seconds (outer layer only) | ASTM F 1939 |

| | | | | |
|---|---|---|---|---|
| | EN 1486 | $RHTI_{24}$ (heat transfer - radiation)<br>Radiant Heat: 40 $kW/m^2$<br>(done after mechanical pre-treatment as specified in annexure A) | $RHTI_{24} \geq 120$.<br>(component assembly) | EN ISO 6942 |
| Heat transfer (flame exposure) | NFPA 1971 | TPP (Thermal protection performance)<br>heat flux: 84 $kW/m^2$ | TPP ≥ 35.0<br>(component assembly) | ISO 17492 |
| | EN 1486 | HTI24 (heat transfer - flame)<br>Heat flux: 80 $kW/m^2$ | $HTI_{24} \geq 21$ s<br>(component assembly) | ISO 9151 |
| Heat transfer (conductive exposure) | NFPA 1971 | Conduction and compressive Heat resistance (CCHR)<br>Temperature: 280°C<br>Shoulders tested at 2psi; knees at 9 psi | Time to $2_{nd}$ degree burns ≥ 25 s<br>(component assembly) | ASTM F 1060 |
| | EN 1486 | Heat transfer : conductive<br>Temperature of 300°C<br>No applied pressure | Threshold time shall be ≥ 15 s.<br>(component assembly) | ISO 12127 |
| Flame resistance | NFPA 1971 | Flame resistance | After flame not more than 2 s<br>no melting or dripping<br>(individual layers) | ASTM D 6413 |
| | EN 1486 | Flame spread | no hole formation, no flaming/molten debris, after-flame time ≥ 2 s, afterglow ≥ 2 s | ISO 15025 |

| | | | | |
|---|---|---|---|---|
| | | | (component assembly) | |
| Hot atmosphere | NFPA 1971 | Heat resistance<br>(Temperature: 260°C exposure time: 5 min) | Shall not melt, drip, separate, or ignite Shrinkage ≤10% (Individual layers) | ASTM F2894 |
| | EN 1486 | Heat resistance Temperature: 255 °C (± 10 °C)<br>Exposure time: 5 min | No melting, dripping, or ignition; shrinkage 5 % (component assembly) | ISO 17493 |
| Wet flex Test | NFPA 1971 | Specimen immersed in hot water for 15 minutes followed by flexing for 1000 cycles | No sign of cracking or delamination | Procedure specified in NFPA 1971 |
| Adhesion after wet flex | NFPA 1971 | Tape Method (using a tape with adhesion value of 4.8 N/ 25 cm to 6.2 N/25 cm) | No evidence of separation or removal of the surface coating | Procedure specified in NFPA 1971 |

At present, the outermost layer of fire proximity clothing of requisite standard (as listed in the above table) is not being manufactured in our country. Further, very few companies internationally manufacture this aluminised glass fabric, which are able to qualify the stringent NFPA 1971 standard requirement. Considering the huge requirement of proximity firefighting suits in both Defence and civil sector, its indigenization is highly desirable. Gentex is one of the players, whose outermost layer meets the requirement of both these standards.

## 1.4 FABRIC PROPERTIES

The properties of most commonly used fabric in heat resistant clothing/Firefighting suits are listed in Table 1.2.

**Table 1.2** Thermal properties of Fabric

| **Fabric** | **Density** $\rho$ (kg $m^{-3}$) | **Specific Heat** $C_p$ (J $Kg^{-1}K^{-1}$) | **Thermal Conductivity** k (w $m^{-1}K^{-1}$) |
|---|---|---|---|
| **PBI** | 323 | 1300 | 0.05 |
| **Nomex-IIIA** | 286 | 1300 | 0.04 |
| **Aralite** | 1380 | 1200 | 0.13 |
| **Kombat** | 1384 | 1420 | 0.179 |
| **Comfort Zone** | 1295 | 1325 | 0.144 |
| **Inner Liner** | 600 | 1300 | 0.05 |

Nomex IIIA is a composition of 93% Meta-aramid, 5% Para-aramid (Kevlar) and 2% anti-static carbon fiber.

## 1.5 SKIN LAYERS

The biggest organ in the human body, the skin serves as the body's cooling and insulating barrier, barrier against disease, and barrier against germs. The epidermis, dermis, and subcutaneous tissue are the three primary layers of skin that make up the skin (Fig. 1.6).

The epidermis, which is the outermost layer of skin, has a usual depth of 75 to 150 μm. The outer layer of the epidermis's dead cells are replaced by new ones in the basal layer. The dermis, which is one to four millimetres thick and houses the vascular,

neurological, lymphatic, and hair follicle components, is located beneath the epidermis (SFPE Guide 2). Generally speaking, cells cannot recover when heat damage penetrates deeper than the depth of a hair follicle. Subcutaneous tissue, which is the last layer, is primarily made up of fat and connective tissue but also includes blood vessels and nerves. Because fat serves as an insulator, it has a significant impact on how the body regulates temperature.

.

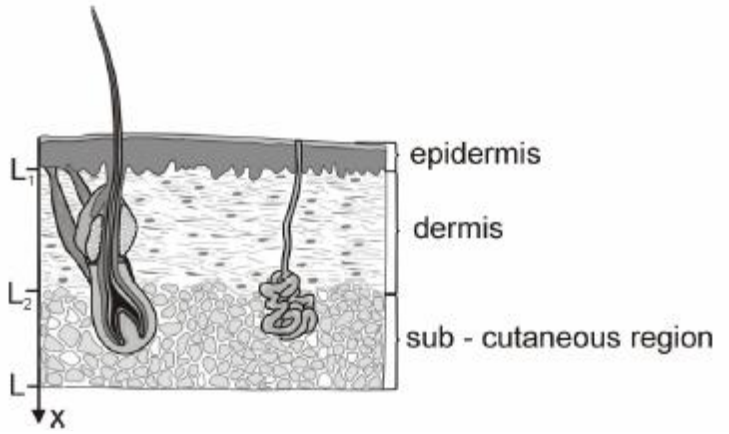


**Fig. 1.6** Skin Layers

## 1.6 SKIN BURN TYPES

The degree of skin damage is ranked in order to assess skin burns. Skin burns can be rated on a variety of scales, the most popular of which being the first, second, or third degree burn.

**1.6.1 First Degree Burn:** First-degree burns are the most superficial. In this instance, just the epidermis is impacted by the heat damage. First-degree burns show up physically as redness and some pain, but not blistering. As the skin recovers and the basal layer's new cells replace the dead ones, the epidermis will flake and peel.

**1.6.2 Second Degree Burn:** When the epidermis is damaged, a second degree burn happens. A second-degree superficial burn does not cause dermal damage. The injury is classified as a deep second-degree burn if the dermis is harmed. The skin will hurt

and appear red, blistering, and wet physically. If the burn is serious, a faint white colour will show through the blisters.

**1.6.3 Third Degree Burn:** Third degree burns happen when the epidermis and dermis are completely necrotic. This burn goes below the depth of the hair follicle. Perforations may also reach the subcutaneous layer. The skin will seem gray, burned, and have a leathery appearance since it cannot repair itself. Often, the burn victim will not feel anything at the burn site.

**1.6.4 Fourth Degree and Beyond:** The grading system does go up to a sixth degree, despite the fact that discussions of burns are typically limited to first, second, and third degrees. Skin grafts are necessary for the recovery of patients with burns of the fourth degree. Burns that are classified as fifth degree involve muscle damage. Burns of the sixth degree harm the bone.

## 1.7 PREDICTING SKIN BURN

The typical temperature of human skin is 32.5˚C; temperatures higher than 44˚C cause burning. These techniques ignore conduction and convection and view radiation as the only type of thermal injury. They base their model on the assumptions that skin is opaque, subject to continuous thermal injury, begins at 32.5˚C, and is a semi-infinite solid. Henrique's Damage Integral model is considered as the primary model to be followed in the ASTM F1930 standard, the guiding document for this project.

## 1.8 BENCH SCALE TESTS

Following are the main bench scale tests.

ASTM D 4108, NFPA 1971 TPP and NFPA 1977 RPP.

### 1.8.1 ASTM D 4108: Standard for Open Flame Test Method for Thermal Protective Performance of Clothing Materials

The process described in ASTM D 4108, which was taken out of print in 1996 (Gagnon), is remarkably similar to the one employed in NFPA 1971 for assigning

Thermal Protective Performance (TPP) ratings. Samples of material are subjected to a brief exposure to a convective heat flow of 84 kW/m2 (2 cal/cm2s) during the test. Using a Meker or Fisher burner, the sample is heated from the bottom. An ASTM E 457-compliant copper calorimeter is used to quantify the amount of heat passed through the material. It is placed above the sample.

A 6.4 mm spacer is needed for single layers in order to create an air gap between the sample and the sensor. The air gap is not necessary for samples with many layers (ASTM D 4108). A shutter that is cooled by water regulates the exposure time. Since the shutter is water cooled, no heat from the burner may reach the sample before the test starts. The curve created by Stoll and Chianta is used with temperature data from the copper calorimeter to forecast the occurrence of a second-degree burn. The intersection point can be found by superimposing the Stoll and Chianta curve on the copper calorimeter temperature curve. The beginning of the exposure (shutter open) must coincide with the zero time point of the Stoll and Chianta Curves. Second-degree burns are said to occur at the time coordinate at the place where the two curves connect (ASTM D 4108). Given that the Stoll and Chianta curve can only be applied in situations when a square wave heat flux exposure, such as the one that was applied to the sample, this criterion could initially appear to be quite fair. The fact that the heat flux incident on the copper calorimeter is not a square wave, however, is a less evident feature.

After the exposure is complete, the heat flux that reaches the copper disk has an approximately rectangular shape, but it does not reach its maximum value right away. Instead, it gradually decreases to zero. Multiple-layer tests will result in an even more attenuated heat flow that is not square in shape. This demonstrates the inherent ambiguity in using this kind of burn prediction criterion. Although it's unclear how much of an impact this has on the outcomes, it does cast doubt on how accurate a burn prediction is in comparison to an actual burn.

### 1.8.2 NFPA 1971: Structural Firefighting Protective Clothing

The NFPA 1971 offers design guidelines for outfits used in structure firefighting. It consists of multiple tests to gauge the material's strength and the quality of the seams, as well as a TPP test to gauge the level of thermal protection offered. The NFPA does not enforce codes, thus protective ensembles are exempt from this requirement. It offers the customer a certain amount of assurance and denotes a minimal degree of durability and heat protection. The criteria for thermal protection are more significant for this literature assessment.

The ASTM D 4108 test and the TPP test utilized in NFPA 1971 are comparable in nature. It combines two types of burners—a pair of Fisher or Mekker burners for convective heat flux and a bank of quartz lamps for radiant heat. A water-cooled Gardon type heat flux transducer must be used to verify that the sample's total heat flux incident is 2.0 cal/cm$^2$ ± 0.1 cal/cm$^2$ (84 kW/m$^2$± 4 kW/m$^2$ ). Six-by-six-inch (15.2 cm by 15.2 cm) material samples are placed on a mounting plate with a four-by-four-inch square hole cut out to reveal the material. Heat is applied from below, with specimens positioned horizontally. The Stoll Criterion is used to calculate the time to second degree burn when testing a sample of material. The total TPP (Thermal Protective Performance) rating is determined by the below equation.

$$TPP = F * T \qquad (1.1)$$

Here:

F = total heat flux in cal/cm $^2$

T = time in seconds for intersection with the Stoll burn criterion

As per NFPA 1971 the entire clothing consisting of outer shell, moisture barrier and thermal liner have a TPP rating at least 35.0 cal/cm$^2$ (1450 kJ/m$^2$ ).

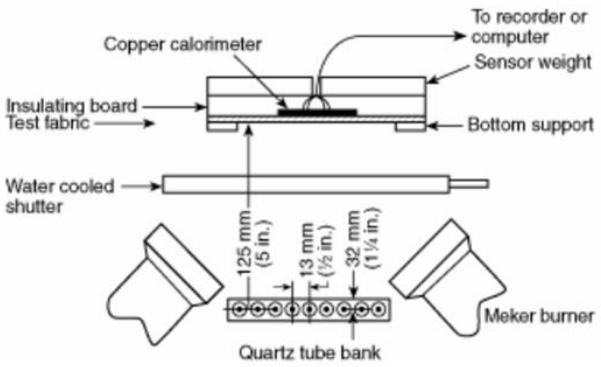


**Fig 1.7** Set-Up for TPP test procedure as per NFPA 1971

### 1.8.3 NFPA 1977: Guidelines for Equipment and Protective Clothes for Fighting Wildland Fires

Compared to their structural firefighting counterparts, ensembles and equipment used to combat wildfires and wildland urban interface fires must meet distinct specifications. NFPA 1977 aims to meet these various requirements. Because they are usually moving around a lot while fighting outdoor fires, firefighters need a lightweight ensemble that shields them from radiant exposure. NFPA 1977 mandates the Radiant Protective Performance (RPP) test in lieu of the TPP test as required by NFPA 1971. A bank of quartz lamps providing a heat flux of 0.5 cal/cm $^2$ ±0.1 cal/cm 2 (21 kW/m 2 ±4 kW/m 2 ) is exposed to a portion of material in this test. By subjecting the bare copper calorimeter to the radiant panel for ten seconds, the incident heat flux is ascertained.

The heat flux can be determined using equation 1.2.

$$q_r = \rho c_p \, \delta\Delta \, T/\Delta \, t \qquad (1.2)$$

The material samples used are 3" by 10" (7.6 cm by 25.4 cm) and are held vertically in a specimen holder that has a cut-out measuring 2.5" by 6" (5.7 cm by 14 cm) that exposes the substance. According to NFPA 1977, 1998 textiles used to combat wildland fires must have a minimum RPP value of 7.0 cal/cm$^2$ (290 kJ/m$^2$).

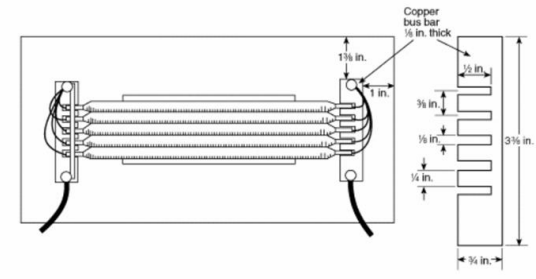


**Fig 1.8** NFPA 1977 RPP Test by Quartz Lamps

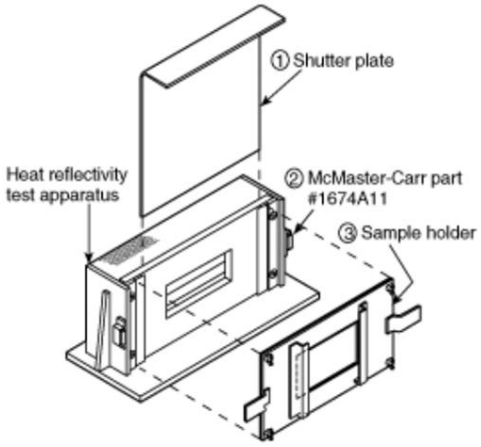


**Fig 1.9** Specimen Holder Assembly for NFPA 1977 RPP Test (NFPA 1977, 1998)

## 1.9 LIMITATIONS OF BENCH SCALE TEST

Note that current lab-scale testing methods only examine a small portion of the material. Seams, reflective patches, and structural elements of combat equipment such as hook-and-loop fasteners and zippers can adversely affect the protection provided, and this issue was not addressed in these laboratory tests. The combustion criteria presented by Stoll and Chianta apply only for use with square wave heat fluxes. It has been found that deviations from the square wave invalidate the combustion criterion. However, this combustion standard is used for both his NFPA 1971 and NFPA 1977. These shortcomings are not emphasized to render clinical testing irrelevant or obsolete.

These are highlighted to illustrate some of the complexities involved in thermal materials testing problems. Laboratory-scale tests are very useful and can be used to benchmark the thermal protection of body armour. Note that these tests do not necessarily correlate strongly with the burn times that occur when exposed to real fires. However, it can be a useful reference for different materials comparison.

## 1.10 FULL SCALE TESTS

While manikin testing is far more costly and involved than bench scale testing, it can yield unique and occasionally more valuable data. There are very few institutions and organisations where manikin thermal testing conducted.

DuPont's Thermo-Man, North Carolina State University's Pyro-Man, and the University of Alberta test. This section also covers Thermo-Leg ®, an instrumented leg test that is somewhat full scale. A more precise estimate of a protective suit's reaction to a fire exposure can be obtained by full scale testing. The majority of mannequin experiments that are now available aim to replicate a "ideal" flash fire exposure of 84 $kW/m^2$ (2.0 $cal/cm^2*s$). This represents an approximation of the heat flux that a firefighter might encounter during a brief (often less than five seconds) containment in a strong flash fire. Even for brief periods of time, its value is greater than what the majority of firemen will ever encounter. While flash flames can cause a far more severe thermal shock, most everyday firefighting use involves far lower heat fluxes. This has been demonstrated in various studies. Table 1.3 shows several different flash fire exposures and the resulting measured heat fluxes.

**Table 1.3** Flash Fire Heat Flux

| | |
|---|---|
| Explosions (Mine) | 130-330 kW/m2 |
| JP-4 Fuel Fires | 67-226 $kW/m^2$ |
| Severe Post Flashover Fires | Approx. 180 $kW/m^2$ |
| Flash Fire (Propane) | 160 $kW/m^2$ |

There has always been significant discussion about the significance of these greater heat flux levels and the viability of creating a test to replicate such a severe exposure. This is noted here to draw attention to the possibility that the exposures utilized in the current mannequin studies are not representative of the real-world situation they are meant to simulate (Torvi, 1997). LeBlanc investigated potential shipboard fire scenarios for the Navy. Navy personnel wearing protective garments will most likely be subjected to these kinds of design fires (LeBlanc, 1998). LeBlanc discovered that the shipboard fires that are most likely to happen are:

(i) Spaces for Machine Areas: The most common places for machine rooms to catch fire are those housing engines, steering gears, generators, auxiliary machines, repair shops, and other machinery rooms. the profusion of flammable liquids near sources of fire, such as sparks, cutting, welding, and electricity.

(ii) Supply Areas- Mess halls, laundry rooms, galleys, and storage areas are examples of spaces with a lot of solid fuel sources and not a lot of liquid fuel. In these places, grease fires are the most frequent type of fire.

(iii) Habitable Areas- Beds and other flammable items are frequently seen in the quarters of crews and officials. It is anticipated that smoking accessories, arson attempts, or defective wiring will serve as ignition sources.

(iv) Deck Storage Spaces- Topside activities are changing, making it challenging to categorize these areas. Painting and cleaning will probably be the main causes of fires. The most dangerous fire source will come from an airplane collision or gasoline spilled during refuelling.

LeBlanc concluded that the most dangerous fire situations were those involving pools and jets, which most likely involved flammable liquids like fuel or hydraulic fluid. At distances of 0.5-4.0 m, the maximum radiative heat fluxes from jet flames were found to range from 200-8.0 $kW/m^2$. At a distance of 5.5–20 meters, the radiative heat fluxes from huge pool fires were found to be 80–3.0 $kW/m^2$.

Manikin testing sheds light on the effects of body geometry as well. Make maps of places that are prone to fire and compute fire predictions for every sensor. To measure the amount of heat transported through the suit and convert the heat flux data

to skin temperature, each of the three tests requires a heat flux transducer of some kind. The Enrique integral of burn injury is then utilized to determine skin burn based on skin temperature. Although numerous attempts have been made to use mannequin testing as a measure of real-world performance, they are currently primarily used for comparison. The time to first, second, and occasionally third degree burns is typically used to compare two suits rather than being taken as an absolute.

The goal of current research is to create tests that can replicate these design fires more precisely. The link between actual full-scale testing and the real-world phenomena it models has not received much attention. Still, the full-scale manikin test yields a wealth of valuable data that lab-scale testing is unable to detect. Less uncertainty exists regarding the flame's spectral emission peak wavelength because the exposure is carried out by a turbulent diffusion flame produced by a gas burner. Additionally, the structural components of protective apparel, including seams and zippers, can be examined using manikin tests.

### 1.10.1 Thermo Man

E. I. du Pont de Nemours and Company developed the Thermo-Man test to evaluate the relative thermal protection provided by its protective clothes, specifically Nomex apparel. ASTM F 1930 Standard describes the test's specifications. The manikin must include at least 100 sensors with a response time of less than 0.1 seconds and the ability to measure incident heat fluxes of up to 4.0 cal/cm$^2$ (167 kW/m$^2$). Propane is the fuel, and according to ASTM F 1930, the delivery system must be able to expose the fuel to 2.0 cal/cm$^2$ (84 kW/m$^2$) for at least 5 seconds.

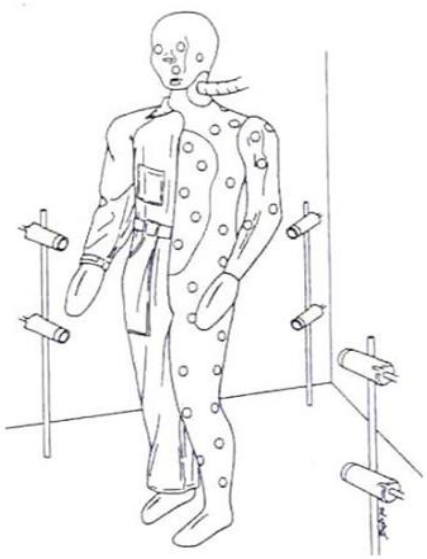

**Fig. 1.10** Set-Up of Instrumented Manikin (ASTM F 1930)

Thermo-Man's sensor type is not widely documented, at least not in the public domain, and the author could not locate much information about the design and manufacturing of the sensors. It is known that they were formerly made of a thermoset polymer with a thermocouple embedded just below the surface. The material's heat response was intended to be comparable to that of skin. Since the implanted thermocouple's location was so sensitive to it, the inverse method used to estimate incident heat flux was prone to inaccuracy.

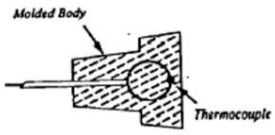


**Fig. 1.11** Sensor for Thermoman

### 1.10.2 Thermo Leg

E. I. du Pont de Nemours and Company conducted a test called Thermo-Leg that is comparable to the Thermo-Man test. An instrumented moving leg apparatus that

mimics running is called the Thermo-Leg test. Four enormous propane torches are used to provide diffusion flames that provide heat to the leg. The leg experiences average heat fluxes of 2.0 cal/cm$^2$ (84 kW/m$^2$). The leg's action is engineered to replicate the trajectory of an ankle in a runner, together with the stride's frequency cycle. Leg running at 1.1 cycles per second results in an average running speed of 3–4 m/s. Running at 9.8 feet per second is the result.

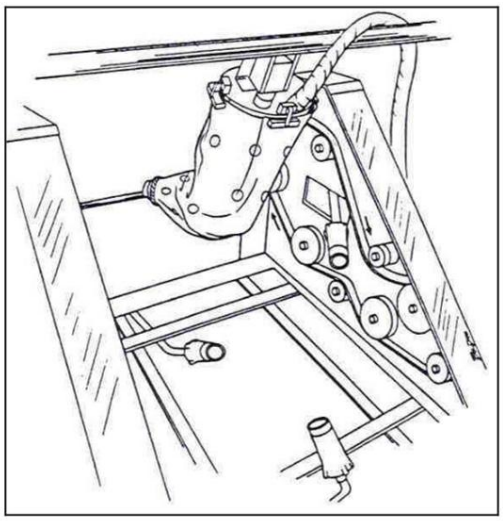

**Fig. 1.12** Thermo-Leg Apparatus

### 1.10.3 Pyro Man

Similar to the Thermo-Man® test, the Center for Research on Textile Protection and Comfort at North Carolina State University uses an instrumented mannequin test. The mannequin's heat flux transducers determine the total incident heat flux both with and without protective clothes. Measured heat transmission through a test garment is used to simulate the skin's reaction and forecast burn damage. Prior to recently, embedded thermocouple sensors were employed for the Pyro Man test; however, copper disk sensors were used instead.

Grimes designed copper sensors were based on an energy balance on a copper disk. The net heat flux calculated:

$$\dot{q}'' = \rho c_p dL \frac{dT}{dt} + h(T - T_\infty) + \dot{q}''_{condlosses} \tag{1.3}$$

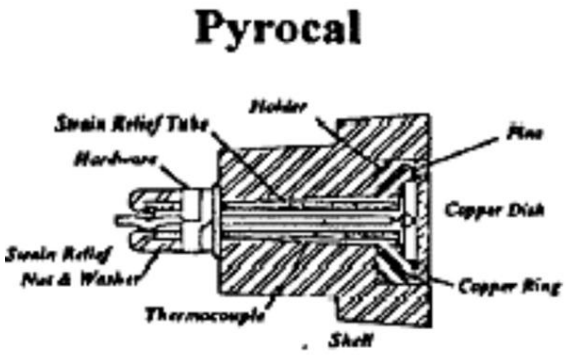


**Fig. 1.13** Grimes developed Copper Slug Sensor

The differential heat balance in equation 1.3 is used to compute the total incident flux to the sensor. An alternative to the copper slug sensor was a water cooled version that functioned by sensing the temperature differential of water moving in and out of the area under a copper disk.

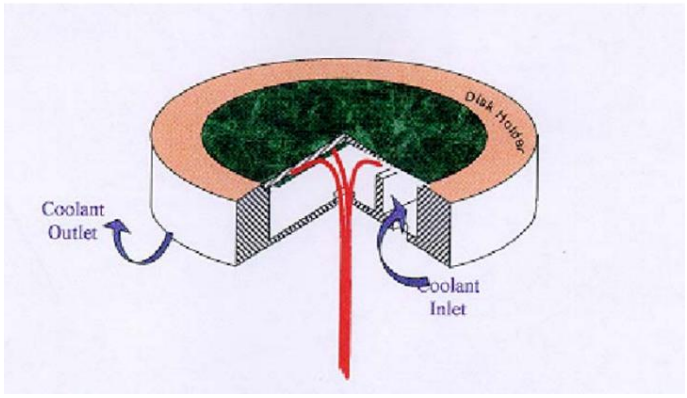


**Fig. 1.14** Pyro Man Water Cooled Sensor

### 1.10.4 Alberta University Test

Alberta University conducts tests with a size 40 instrumented manikin constructed from fiberglass. Heat fluxes of 67–84 kW/$m^2$ (1.6–2.0 cal/$cm^2$ *s) are usually produced by flame exposures for a length of 3-4 seconds. One hundred and ten skin simulant sensors monitor heat fluxes. These sensors are constructed from an inorganic substance known as "Colorceran," which is composed of asbestos fibers, calcium, aluminum, silicate, and binder. The substance that is frequently used to create the top layer of chemical lab benches is called "colorceran." Table 1.3 shows that the material's density, thermal conductivity, and specific heat values are not comparable to those of skin. Nevertheless, the thermal diffusivity, the product of the three and the most significant of all, is quite similar to the value of skin. The way the sensors function is by simulating the heat flux into the skin. Temperatures are recorded by a flat thermocouple held onto the surface by an epoxy-phenolic adhesive (Dale et al, 1992). After the mannequin's sensors are attached, flat black high temperature paint is applied to the entire object. Calculating heat fluxes involves applying a modified version of equation 1.3. The incident heat flux can be calculated by the known values of simulant properties and temperature at the skin surface. Heat transfer into the skin is modelled based on the skin model of Mehta and Wong, and Henrique's burn damage integral model is used to predict the burn.

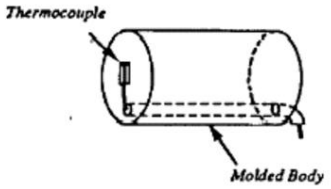


**Fig.1.15** Alberta University Skin Simulant type Sensor

**Table 1.4** Skin thermal Properties and Sensor by Alberta

| Property | Human Skin | | Skin Simulant |
|---|---|---|---|
| | Epidermis | Dermis | |
| k (W/m*K) | 0.255 | 0.523 | 0.97 |
| ρ (kg/$m^3$) | 1200 | 1200 | 1877 |
| c (J/kg*K) | 3598 | 3222 | 1205 |
| kρc ($J^2/m^4*^oC^2*s$) | $1.1*10^6$ | $2.0*10^6$ | $2.2*10^6$ |
| √ kρc ($J/m^2*^oC*s^{1/2}$) | 1050 | 1414 | 1483 |

## 1.11 CONFIGURATION OF THESIS

The thesis consists of six chapters which are summarized below:

**Chapter 1:** This chapter provides an overview of the field of research and its technological significance.

**Chapter 2:** This chapter encompasses the information about contributions and development in the field of fire suit testing by different researchers. It provides a comprehensive review of the available literature on the research topic. It discusses the current state of knowledge in the field and identifies the gaps in the existing research. The chapter also introduces the research gaps and the objectives of the study.

**Chapter 3:** This chapter describes the Modular Burn chamber (enclosed space built from fire-proof materials). Provisions for manikin and cable routing and various equipment that were used in the study.

**Chapter 4:** Analysis of the manikin heat flux and temperature distribution. Validation and parametric investigation.

**Chapter 5:** It includes the results of experimental investigations as well CFD analysis and parametric investigations.

**Chapter 6:** highlights the important conclusions drawn from this work and the scope for further research in this field.

**Chapter 2**

# LITERATURE REVIEW

The chapter reports the findings of the comprehensive literature survey. There are limited literatures focused on the Performance Prediction Modelling and Thermal Analysis of Heat Resistant Clothing. So, this work is very young from the literature point of view.

## 2.1 Influence of moisture on the performance of fire suits

Su et al. [8] reviewed the thermal protective performance of firefighter's clothing under high temperature and high-humidity condition. They discussed the distribution of moisture in a real fire situation as well as the rules of moisture's influence on thermal protection. Various assessment techniques are employed to determine how moisture affects the performance of thermal protection.

In order to ascertain the textile characteristics needed in numerical techniques of heat and mass transport through textiles, Neves et al. [10] established methodologies and experimental procedures. The presence of water in the fibers and the impact of their hygroscopic qualities were taken into consideration when defining experimental methods that enable the estimation of all necessary parameters. Values for textile thickness, fiber fraction, and tortuosity are typically required for numerical models. Additionally, understanding of boundary conditions, such as mass transfer coefficients and convective heat, is necessary. It was demonstrated that the predictions were accurate when the acquired parameters were included in a numerical model and numerical predictions of temperature and humidity were compared with experimental data collected during tests of fabric evaporative resistance.

## 2.2 Impact of air gap on fire suit

Using the sophisticated CFD technique, Tian et al. [9] created a 3D finite volume model to simulate the transient heat transfer through a flame manikin situated in a combustion chamber. They used the Donghua flame manikin system to conduct point-by-point comparisons between the model and real trials to validate it. The model

was then used as a foundational model to study the heat transmission through a streamlined protective gear system. Using fabric as a 3D medium, single- and multi-layered apparel with contact combinations were replicated. The findings showed that when it came to reducing heat transfer to human skin, the 6.35 mm air gap was more important than the single layer fireproof clothing. The moisture barrier in the multi-layer garment system provided the best thermal protection during a flash fire. The temporal heat flow and temperature data may be used to improve fabric properties and conduct additional study on burn injury prediction.

### 2.3 Performance of multi-layer fire suit

Wang et al.'s study [5] examined a number of exemplary outer shells, as well as comfort lining textiles, moisture barriers, and thermal barriers. The experimental findings showed that each component layer fabric's average water vapour transmission rate (WVTR) had the following order: comfort lining > outer shell > heat barrier > moisture barrier.

### 2.4 Numerical Analysis and CFD Modelling

Miao et al. [17] simulation research indicate the followings. (1) The increase in heat flux intensity has the most substantial impact on the proportion of skin burns. (2) The proportion of skin burns generally increases with the increase in heat exposure duration. When the heat exposure duration is long, burn injuries tend to concentrate on the upper body because of the accumulation and increase in hot airflow. (3) With the increase in clothing thickness, the variation in the proportion of first-degree burns on the body's skin surface exhibits fluctuations. The proportion of second-degree burns considerably decreases between clothing thickness levels 1 and 3. (4) No clear pattern was observed in the proportions of skin burns with increasing clothing surface emissivity.

Heat transmission through the fabric-human skin system exposed to both radiant heat and high intensity flame was examined by Udayraj et al. [11]. The amount of heat transfer through four distinct fabric samples is measured through experiments. Using the Dual Phase Lag model of Bio-heat transfer, the temperature distribution

across the different skin layers is computed while taking the temperature-dependent blood perfusion rate in the dermis and subcutaneous layers into account. Within human skin, wave phenomena is seen. Henriques' burn integral relation is used to calculate second degree burn time. Stoll's criterion-based experimental results are compared with second-degree burn times. They advised using DPLMBT to analyse heat transport within human skin after exposure to high heat flux for such a little amount of time.

A computational fluid dynamics (CFD) model was created by Barry et al. [6] to forecast the effectiveness of chemical and steam/fire protective garments. The software calculates phase change, vapour and liquid sorption processes, capillary movement of liquids, diffusive and convective heat and gas/vapor transport, and the variable properties of the many layers of clothing.

In order to model the transient heat transfer that occurs in firefighters' protective gear when they are exposed to flash fires, Ghazy et al. [7] created a finite volume model. The human skin, the air gap between the garment and the skin, and the outer shell, moisture barrier, and thermal liner are the three layers of fire-resistant materials that make up the model domain. As a function of time, predictions were derived for the temperature and heat flow distributions in the skin, air gaps, and fabric layers.

Dagur et al. [14] used k-w turbulence model using Ansys Fluent for the analysis. ICEM CFD used for meshing.

Arora et al. [15] carried analysis of diffuser using CFD.

### 2.5 Research Gaps and Future Directions

The vast literature survey indicates the following research gaps:

1. **Limited data on multilayer fire suits:** Only fewer data is available on the thermal properties of different new fabrics used for multilayer fire suits.

2. **Lack of CFD model to validate experimental data:** there are very few research papers to validate the experimental data with CFD model by applying various CFD models.

## 2.6 Motivation

The survey reveals that most of the existing studies have been confined to a limited scope of single layer fabric. There is no validation of experimental result with numerical/CFD model is available. The prime concentration of these studies is to evaluate the multi-layered fire suit and validate the results with CFD.

With this objective, this work aims to carry out the "**Performance Prediction Modelling and Thermal Analysis of Heat Resistant Clothing"**.

## 2.7 Scope of the Present Work

The scope and primary objectives, which contribute to the novelty of this work, include:

1. To develop the experimental set up for manikin heat flux analysis.
2. To determine the temperature variations at different location of the manikin as per ASTM F 1930 standard.
3. To develop the CFD model for the manikin enclosure as per the experimental data.
4. To validate the experimental data with CFD model by applying various CFD models.
5. To carry out parametric investigation with the validated CFD model.

In conclusion, this research paper endeavours to fill the existing gap in Experimental and CFD results. The validation will insure the burn analysis of multilayer fire suits without experiment.

# CHAPTER 3

# RESEARCH METHODOLOGY & EXPERIMENTAL SETUP

This chapter describes the methodology used for research work. The experimental setup used for research is explained in detail.

## 3.1 RESEARCH METHODOLOGY

The following steps followed:

- Study of various types of Protective clothing with regards to Analysis.
- Study of various types of Heat analysis chamber
- Design and fabrication of Heat analysis chamber.
- Carried out experimental studies to record various performance parameters.
- CFD Performance prediction modelling of heat resistant clothing.
- CFD analysis (Thermal) and simulation studies of heat resistant clothing
- Validated the computational fluid dynamics (CFD) against experimental data or/ data available in the literature.
- Parametric investigation using CFD and optimize the design.

Conduction Equation (Cartesian) [12] has been used for heat flux analysis

$$\frac{\partial}{\partial x}\left(k\frac{\partial T}{\partial x}\right)+\frac{\partial}{\partial y}\left(k\frac{\partial T}{\partial y}\right)+\frac{\partial}{\partial z}\left(k\frac{\partial T}{\partial z}\right)+\dot{q}=\rho Cp\frac{\partial T}{\partial t}$$

The standard k-∈ Turbulence Model is used in CFD for calculations which is a set of following equations [13].

for turbulent kinetic energy k

$$\frac{\partial(\rho k)}{\partial t}+\frac{\partial(\rho k u_i)}{\partial x_i}=\frac{\partial}{\partial x_j}\left[\frac{\mu_t}{\sigma_k}\frac{\partial k}{\partial x_j}\right]+2\mu_t E_{ij}E_{ij}-\rho\in$$

for dissipation ∈

$$\frac{\partial(\rho\in)}{\partial t}+\frac{\partial(\rho\in u_i)}{\partial x_i}=\frac{\partial}{\partial x_j}\left[\frac{\mu_t}{\sigma_\in}\frac{\partial\in}{\partial x_j}\right]+C_{1\in}\frac{\in}{k}2\mu_t E_{ij}E_{ij}-C_{2\in}\rho\frac{\in^2}{k}$$

## 3.2 FLAME TEST MANIKIN SYSTEM (FTMS)

Experimental setup consists of Modular Burn chamber which include the following:

- Self-contained, enclosed space built from fire-proof materials.
- Suitable for installation outside or within an interior laboratory space
- Fuel distribution and delivery system to achieve uniform flame front onto manikin
- A pre-designed ventilation system that releases heat from the burning material and provides oxygen for combustion.
- Safety sensors and interlocks built in to safeguard users and equipment
- Safety window in access door and large viewing window in wall
- Mounting provisions for manikin and cable routing as necessary to protect from heat exposure.
- Video monitoring system for safety and visual documentation of flame and garment response.

The fully ventilated, fire-resistant burn enclosure will be provided with viewing window and access door to house the burner apparatus and manikin. The figures below depict the Modular Burn chamber concept illustration. The chamber will be sized to either meet or beyond the minimal dimensions required by the F1930 standard, which are 2.1 x 2.1 x 2.4 meters. This will ensure that there is a consistent flame exposure and enough room for safe movement around the manikin during dressing without the risk of unintentionally jarring and shifting the burners. After the data collection time, the forced air exhaust system will be sized appropriately to enable quick evacuation of combustion gas products and help with cooling.

Gaseous fuel would be safely delivered to the ignition system and exposure torches via a system of propane gas pipelines, pressure regulators, valves, and pressure sensors. For a minimum of five seconds of exposure, this delivery system must be able to produce a uniform heat flux of at least 2.0 $cal/cm^2 \cdot s$ (84 $kW/m^2$).

The burner system must include a safety pilot flame, an ignition pilot flame for every exposure burner, and enough burners to meet ASTM F1930 standards for flame distribution homogeneity while providing the necessary range of heat fluxes.

To provide a consistent laboratory simulation of a flash fire, big industrial-style propane burners with induced combustion air will be placed surrounding the manikin as the flame exposure burners. It is necessary to use and arrange a minimum of eight burners in order to achieve uniformity and the necessary exposure level.

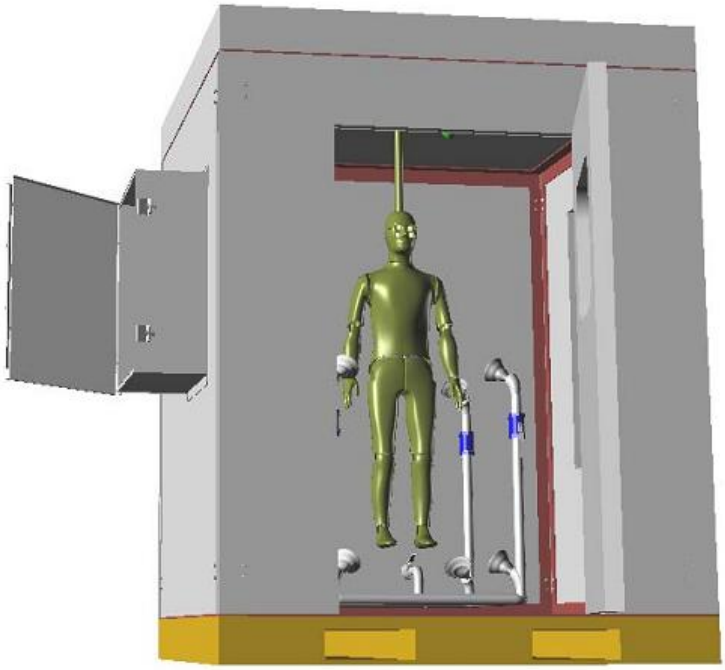

**Fig. 3.1** Modular Burn Test Chamber

The results of the tests will be used for analysis, performance comparison and Burn Injury Prediction of different Fire Protective Ensembles under simulated flash fire.

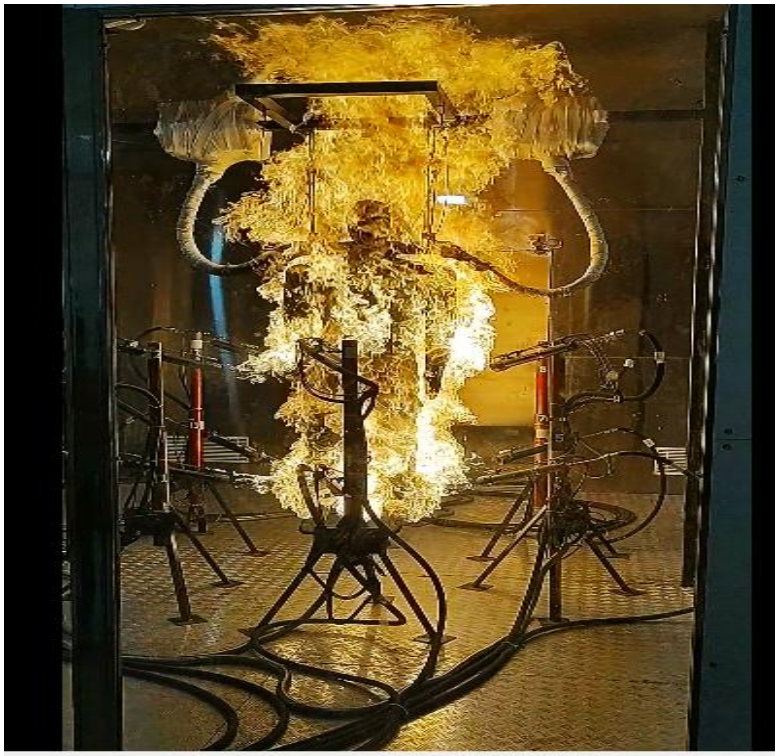

**Fig. 3.2** Flame Exposure on Manikin

A numerical model developed for simulating real life behaviour of fire protective clothing (FPC). Fabric parameters like thickness, geometry etc. and other parameters like thermal and mechanical properties will be incorporated in modelling.

The numerical model analysed and the results compared with the actual experimental data available or the reported literature. An overlap of comparison between the experimental results and the simulation results will validate the numerical model. If the required overlap is not achieved the numerical model will be accordingly modified to correctly predict the real behaviour.

The Manikin was subjected to artificially generated heat flux and the temperature variations at 134 points on the manikin were recorded.

The Manikin used for experimentation was drawn having same configurations as used for the experimentation. The geometry so produced was imported in the ANSYS Fluent. Meshing as well as boundary layer meshing was created on the imported geometry. The CFD modelling was modified according to the experimental inlet heat

flux. The various properties were incorporated. This was done to take care of the distortions in the heat flow field.

In the pre study various models such as k- ε, k- ω, Reynolds stress model to verify the CFD model with the experimental results. It was found that the turbulence model of RNG, k- ε had shown better results and were in accordance with the experimental results.

Once model was finalized, Grid independence test was tested with different mesh sizes was carried out, but the results with 0.7 mm were found to be near to the experimental results.

CFD analysis was carried out to further determine the performance of heat flux at various time intervals

### 3.2.1 MANIKIN

Manikin is a model of human body with specified dimensions that represents an adult human form.

- Manikin body form with jointed hips, shoulders, knees, elbows etc
- High-temperature, non-degrading ceramic-composite body form
- 134 heat sensors evenly distributed over manikin skin surface.
- To reduce penetrations in the test clothing, the mounting support and cable connection are routed from the top of the head, side, or rear of the neck.

### 3.2.2 Manikin Body Form

The 50th percentile manikin body form will be used and will be fully jointed to include the elbows, knees, and ankles. Morphology of the manikin will be based on 3D computer models representative of a 50th percentile Western or Asian male, based on a set of anthropometrics data from several sources.

**Design features a flame proof ceramic-composite body form**

- 134 copper disc calorimeter heat sensors evenly distributed over manikin skin surface
- Manikin will have free-moving joints to simulate walking motion capability using walking motion stand
- Mounting connection at the top of the head or other user-selected location

**Fig. 3.3** Manikin Body Form

### 3.2.3 Heat Flux Sensors

The sensor used for the experiment is skin simulant sensor. The thermocouple embedded, high temperature epoxy sensor represents a variation of the basic slug calorimeter design. It incorporates a thermal resistance layer, an embedded thermocouple and a remaining body of matching thermal-physical properties polymer resin formed in the shape of a circular "plug" (see Fig 3.4). The high temperature epoxy resin is chosen to provide an approximate "skin simulant" response function.

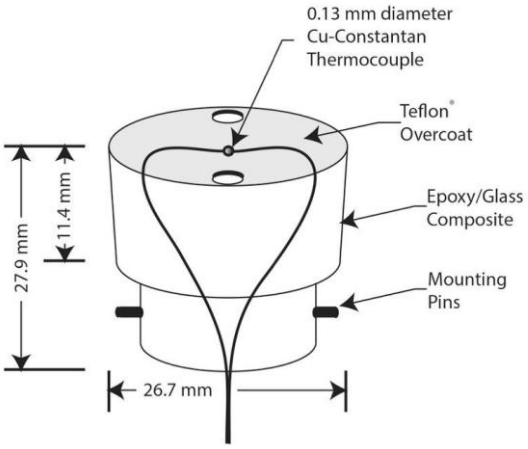


**Fig. 3.4** Heat flux sensor design

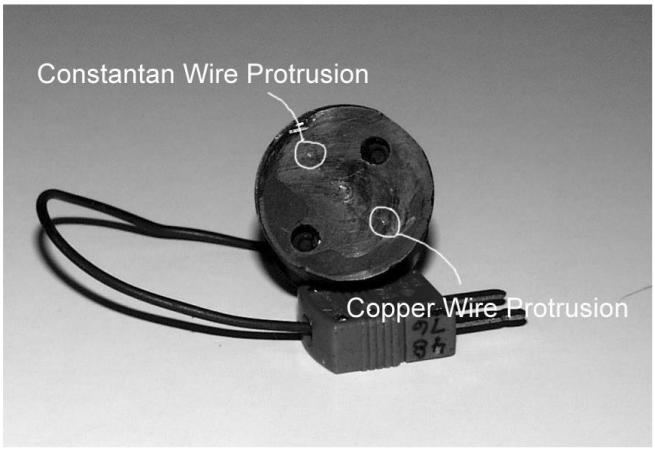


**Fig. 3.5** Skin simulant heat flux sensor

### 3.2.4 Sensor Calibration

The specific nodal depth of the thermocouple from the sensor surface is required in order to evaluate the sensor thermal resistance behaviour, essentially calculating the surface heat flux from the measured temperature using the finite difference method described above. Nodal depth in this context comes from the creation of a discretized problem domain. Essentially, the values of the unknown temperature variable (thermocouple depth locations) are considered only at a finite number of nodal points instead of every point over the region. This is the basis of the finite-difference approach to the solution of the partial differential equations that describes the one-dimensional heat diffusion problem for the epoxy sensor. The

thermocouple essentially resides at one of these nodal points. For simplicity, it is usually the first or second nodal depth point that then defines the remaining internal nodal temperature field. Due to the manufacturing process, the depth will vary from sensor to sensor from the specified 0.305 mm reference depth.

There are accepted straightforward methods to calibrate embedded thermocouple calorimeters of this type. The simplest method to determine the depth of the thermocouple in the epoxy-based sensor is to:

i) Simultaneously expose a specimen epoxy sensor and reference sensor (such as a Schmidt-Boelter or Gardon gauge calorimeter - preferably traceable to a national standard) to a known, single mode heat flux (radiant) (see figure 3.6).

ii) Followed by smoothing the epoxy sensor data with the nonparametric smoothing spline with a smoothing parameter, $\lambda$, of ~0.1, then

iii) Computing and comparing the resulting temporal specimen epoxy sensor heat flux profile to the reference sensor by numerically adjusting the specimen sensor's thermocouple depth (multiplying the reference depth, 0.305 mm, by a calibration factor) until a specified statistical difference (minima) criteria is met.

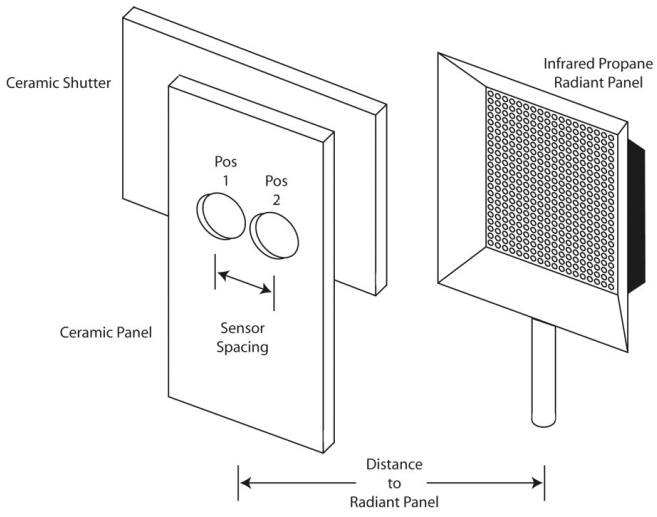


**Fig. 3.6** Schematic of radiant panel calibration unit

### 3.2.5 Data Acquisition System

Flame manikin data acquisition will utilize cabled sensors. Sensor data will be collected at high speed, digitized, and transmitted to a PC user interface running the Burn Model software. Each sensor location's heat transmission will be analyzed to display the appropriate estimated degree of burn damage to human flesh. To display the entire region of the anticipated burn injury, the aggregate of these numbers will be automatically converted to a percentage.

Leads from each sensor will connect to microprocessor control boards mounted inside the manikin. These data acquisition components digitize signals near their source for high accuracy measurements. Cables to the manikin will provide power and communication. This cable will be shielded from flame exposure and will include a connector for manikin handling convenience.

### 3.2.6 Modular Burn Chamber

Modular Burn chamber will include the following:

- Self-contained, enclosed space built from fire-proof materials.
- Suitable for installation outside or within an interior laboratory space
- Fuel distribution and delivery system to achieve uniform flame front onto manikin
- A pre-designed ventilation system that releases heat from the burning material and provides oxygen for combustion
- Safety sensors and interlocks built right in to safeguard users and machinery
- Safety and large watching windows in the access door and wall, respectively
- Mounting provisions for manikin and cable routing as necessary to protect from heat exposure.
- Video monitoring system for safety and visual documentation of flame and garment response.

### 3.3 Conditioning Chamber

Test specimen is conditioned in the conditioning chamber at 21±2 ºC and 65±5% relative humidity for minimum 24 hours before test. Conditioning chamber should be large enough to have good air circulation around the test specimen.

### 3.4 Three Dimensional (3D) Scanning

3D scanner is used for generating 3D image of manikin. 3D scanner provide point cloud data. This cloud data is further meshed and surface created using CATIA. The surface data is further used for CFD purpose using Ansys Fluent.

**Fig. 3.7** 3D Scanning Setup

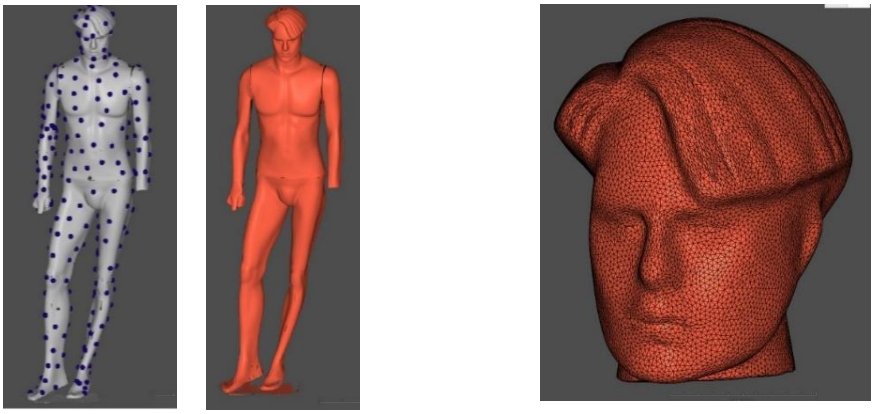

**Fig. 3.8** Scanned Manikin with markers

### 3.5 Experiment Protocol

Single-layer fire suit made of Nomex and cotton were worn. A manikin would typically be clothed, exposed to flames for four seconds, and then left in the room for one hundred and twenty minutes for the experiment. The calibration was determined by exposing the naked manikin test. In accordance with ASTM F1930, suits were initially preconditioned at 65% relative humidity and 28°C. The default heat flux variance is 21, while the average heat flux is controlled at 84 ± 2.5. There is fluctuation in the experimentation procedure, but the nominal fuel flow rate per burner nozzle is 0.006. Propane is used as fuel to create the flux, which is thought to react with a stoichiometric volume of air. Propane has a minimum ignition point of 480°C and an adiabatic flame temperature of roughly 2000°C.

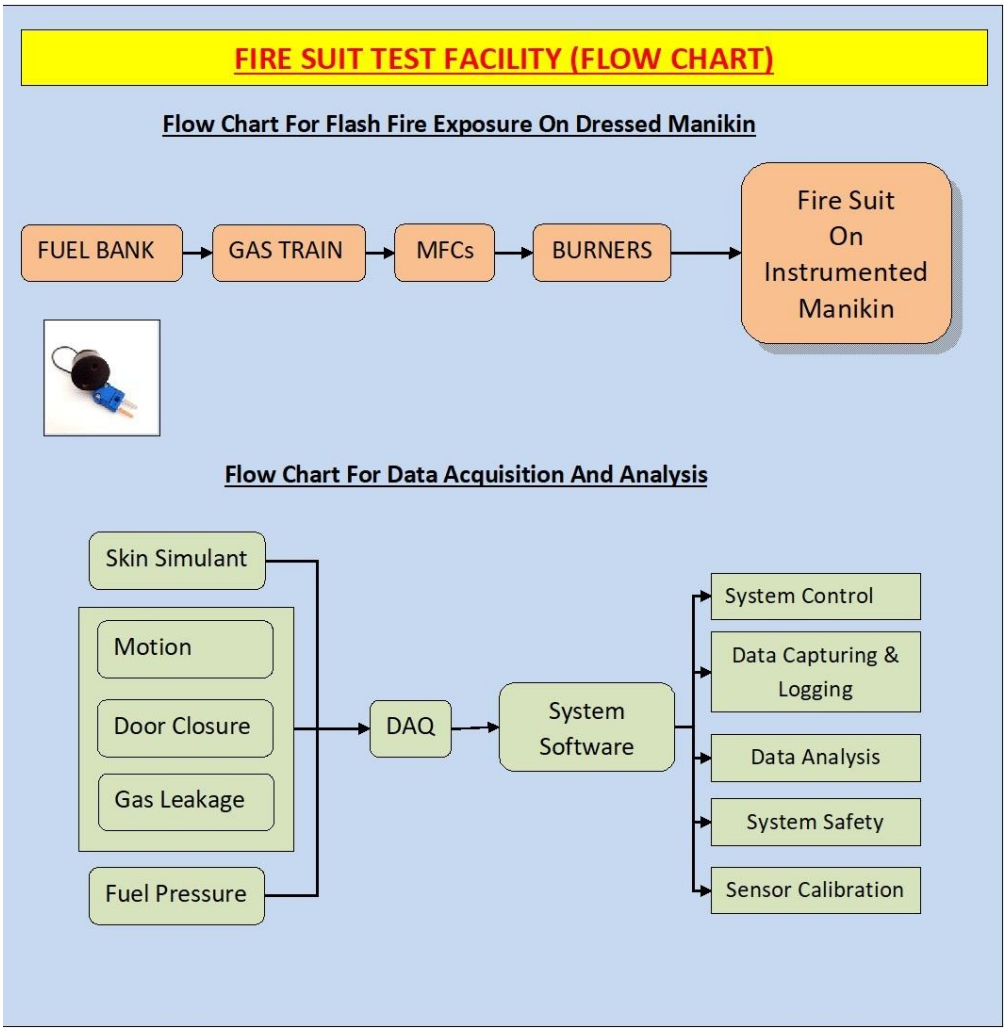


**Fig. 3.9** Flow chart for Fire suit test Facility

### 3.6 Burn injury Assessment

Fig 3.10 shows the burn injury assessment of a multi-layered fire suit.

Average heat flux : 84 kW/$m^2$

Flame exposure time : 8 second

Data acquisition time : 120 second

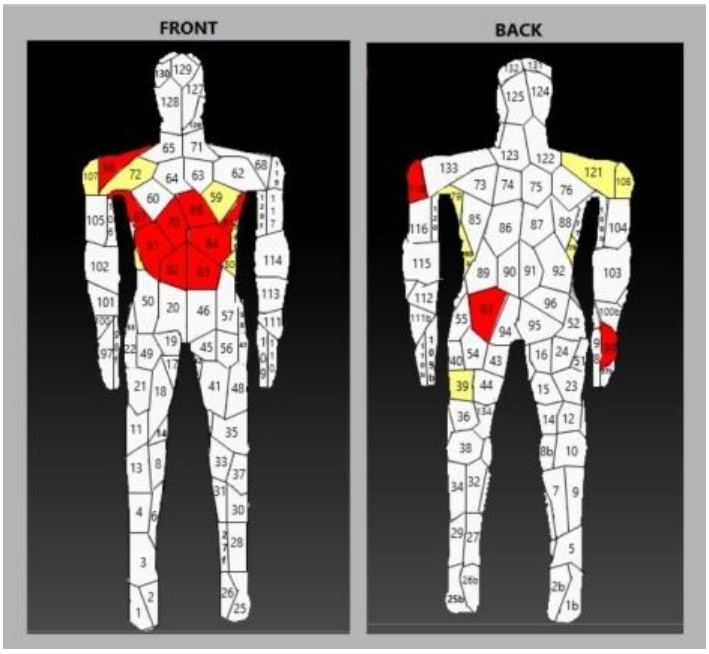


**Fig 3.10** Burn Injury Assessment

Following are the predicted burn injury

2nd Degree burn: 7.78%

3rd Degree Burn: 9.90%

Total Burn Injury: 16.68%

# CHAPTER 4

# CFD ANALYSIS

This chapter compares the simulated values of theoretical model with the experimental results to ensure the applicability of the model for further work. Analysis of the manikin heat flux and temperature distribution has been carried out.

## 4.1 Model for Fire Suit Test Facility

The test facility is commissioned as per ASTM F1930 standard and requires uniform distribution of heat flux across 134 sensors mounted over the manikin. According to the ASTM standard the average heat flux distribution should be 84 kW/m$^2$ ± 5% with flux variance to be less than and equal to 21 kW/m$^2$.

However, conducting the physical trials requires significant time and effort to safely setup, post-process and ventilate the facility. In order to ease these efforts numerical tools such as CFD is adopted to cater the prerequisite.

**Fig. 4.1** Model for fire suit test facility

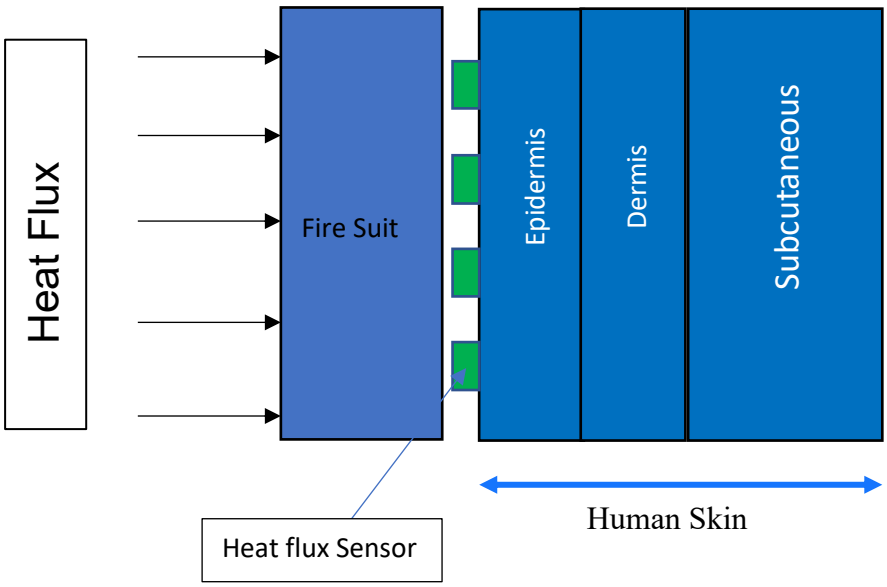

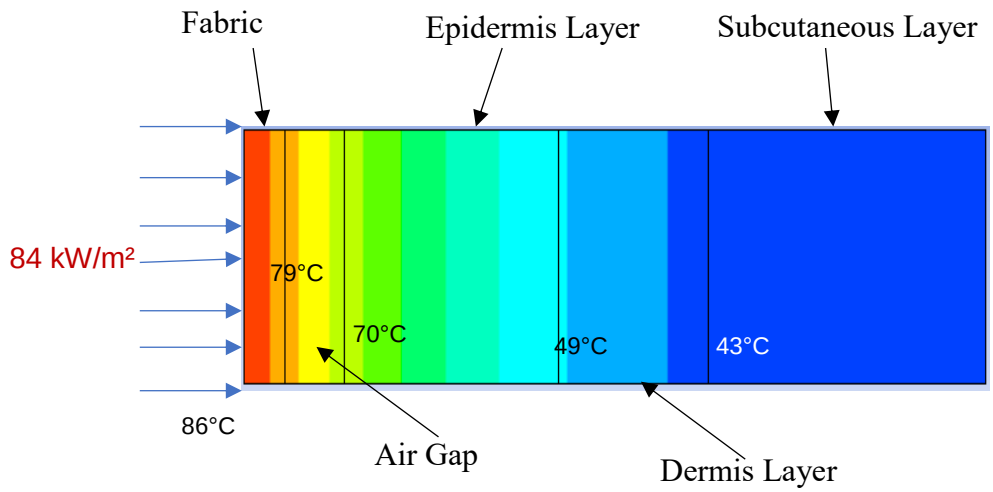


**Fig. 4.2** temperature at different layers

Fig 4.2 shows temperature at different layers of skin and fabric (single layer).

CFD simulations would also provide much needed scientific insights into the flame and heat transfer mechanism around the manikin.

The objective of the CFD analysis that are endorsed for the current study are as follows:

i) Design a suitable approach for CFD modeling and simulation of the experimental test procedure.

ii) Validation of the simulation model with the experimental trials.

iii) Obtain an optimised burner position and orientation, fuel flow rate in parametric CFD analysis of naked manikin test with an aim to achieve the heat flux distribution suggested as in ASTM standard.

iv) Establish a definite set of procedures for CFD modelling, simulation and analysis which will act as a supplement for the corresponding physical trials.

Fluent is used to analyse flow field and heat transfer. Due to time dependent nature of flow the transient, pressure-based solver is utilised to simulate flow and temperature fields.

The standard k-omega SST model is used to simulate the turbulence in the flow including the effect of buoyancy.

### 4.2 Distribution of 134 heat flux sensors

Fig 4.3 shows heat flux sensors distribution over the surface of manikin body.

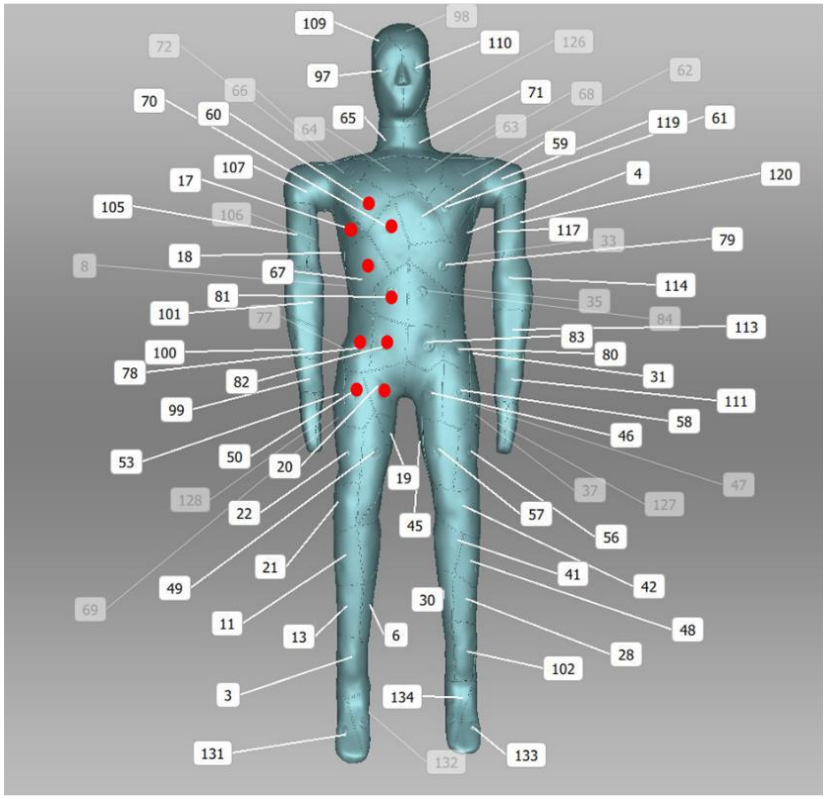


**Fig. 4.3** numbering of heat flux sensors

### 4.3 Mesh Generation

The surface mesh is generated onto the manikin, burner and CFD domain as shown in fig 4.4. The surface elements on the manikin have an edge length of 10.5 mm determined through grid sensitivity study.

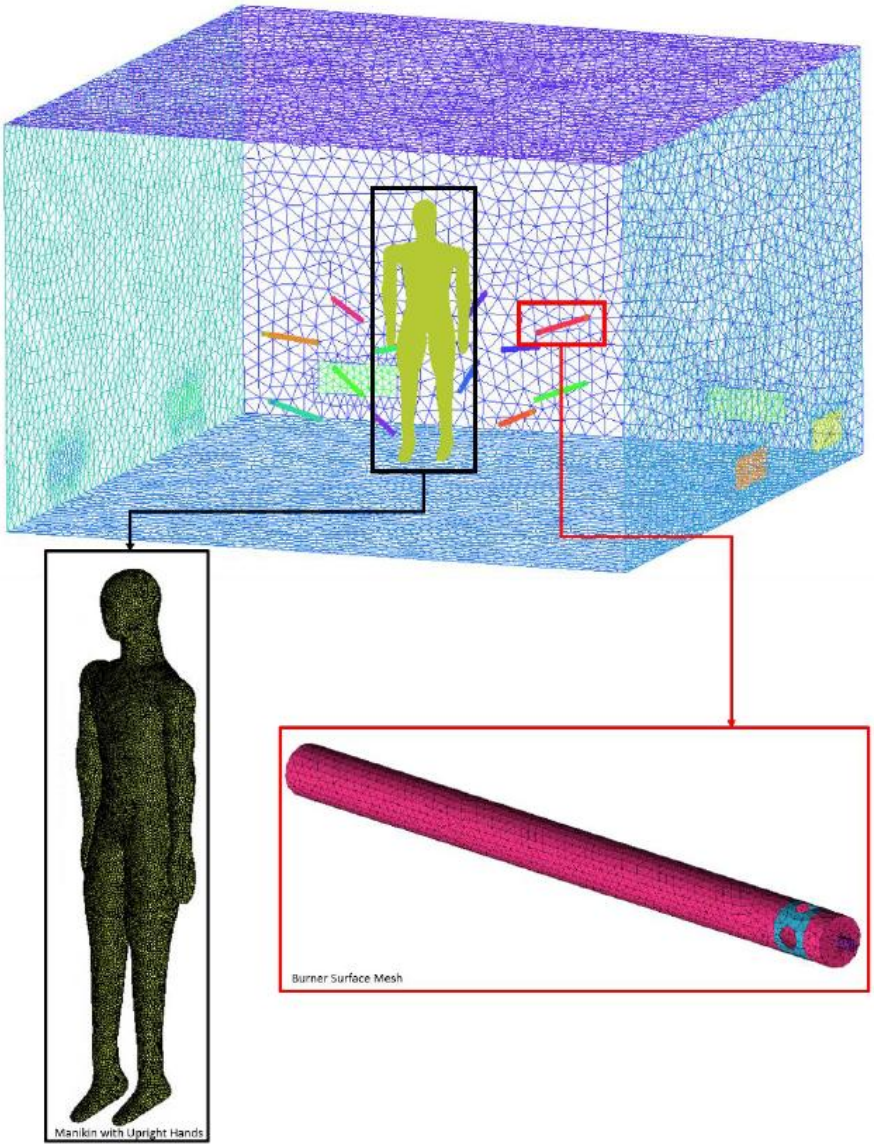


**Fig. 4.4** surface mesh of manikin and CFD domain

The fluid domain is filled with prism elements adjacent to manikin surface and tetrahedral elements elsewhere.

### 4.4 Solver setup and Boundary Conditions

Transient CFD simulation is initiated with zero-gauge pressure and zero freestream velocity field in the flow domain. Inside the test chamber the air and propane have a mass fraction of 1 and 0 respectively at the start of the simulations.

Pressure based transient (incompressible solver) is used and k-omega SST turbulence model applied. Time step 0.01 sec, simulated for 4 second.

Following are the assumptions considered during analysis:

The temperature over the surface of manikin considered is 32 $^0$C.

The Eddy-Dissipation formulation for turbulence-chemistry interaction is used.

The emission pollutant species like NOx, SOx and soot are ignored since we need to evaluate the heat flux only.

### 4.5 Skin Burns Prediction

Henriques proposed the original and, as of right now, most popular model of skin injury, which is a single order Arrhenius expression. The function he proposed, Equation 4.2, displays the rate of epidermal damage can be “modeled as a rate process governed by an activation energy and pre-exponential constant”.

$$\frac{d\Omega}{dt} = P * e^{\left(\frac{-\Delta E}{RT}\right)} \tag{4.2}$$

The function that provides the overall amount of skin damage can be obtained by integrating Equation 4.2.

$$\Omega = \int_0^1 P\, e^{\left(\frac{-\Delta E}{RT}\right)} dt \tag{4.3}$$

The overall damage computed by the above equation indicates the extent of the burn.

Henriques provides the table 4.1 injury parameters.

Table 4.1 Burn Injury Parameters

| Value of Injury Parameter (Ω) | Injury Level |
|---|---|
| 0.53 | First Degree Burn |
| 1.0 | Superficial Second Degree Burn |

The activation energy (ΔE) and pre-exponential term (P) utilized for the burn damage integral will determine the total amount of skin damage that is computed. Henriques (1947) provided values for the activation energy and the pre-exponential term, respectively, of 6.28 x108 j/kmol and 3.1 x 1098 s-1. Many other investigations that have been carried out since Henriques' first work have also used the burn damage integral. These investigations have determined that various input parameter values are suitable. This information is summarized in the SFPE Guide to Predicting First and Second Degree Skin Burns.

Table 4.2- Burn Damage Integral parameters

| Model | Temperature Range °C | Activation Energy, ΔE j/kmol | Pre-Exponential, P 1/sec |
|---|---|---|---|
| Weaver and Stoll | $44 \leq T \leq 50$ | $7.78*10^{8}$ | $2.185*10^{124}$ |
| | $T>50$ | $3.25*10^{8}$ | $1.83*10^{51}$ |
| Fugitt | $44 \leq T \leq 55$ | $6.97*10^{8}$ | $3.1*10^{98}$ |
| | $T>55$ | $2.96*10^{8}$ | $5.0*10^{45}$ |
| Takata | $44 \leq T \leq 50$ | $4.18*10^{8}$ | $4.322*10^{64}$ |
| | $T>50$ | $6.69*10^{8}$ | $9.389*10^{104}$ |
| Wu | $44 \leq T \leq 53$ | $6.27*10^{8}$ | $3.1*10^{98}$ |
| | $T>53$ | $6.27*10^{8}-5.10*10^{5}(T-53)$ | $3.1*10^{98}$ |
| Henriques | All Temps | $6.27*10^{8}$ | $3.1*10^{98}$ |
| Diller and Klutke | $44 \leq T \leq 52$ | $6.04*10^{8}$ | $1.3*10^{95}$ |
| Mehta and Wong | All Temps | $4.68*10^{8}$ | $1.43*10^{72}$ |
| Torvi and Dale | $44 \leq T \leq 50$ | $7.82*10^{8}$ | $2.185*10^{124}$ |
| | $T>50$ | $3.27*10^{8}$ | $1.83*10^{51}$ |

The degree of disagreement between the values of the various models indicates the complexity of the problem and the difficulty of predicting fire damage using simple models. The values of the input parameters differ by orders of magnitude. Burn times for different models do not differ by magnitude order, also there is considerable

variability in the data. Figures 4.5 and 4.6 show the spread of time to 1st and 2nd degree superficial burns produced by various fire damage models.

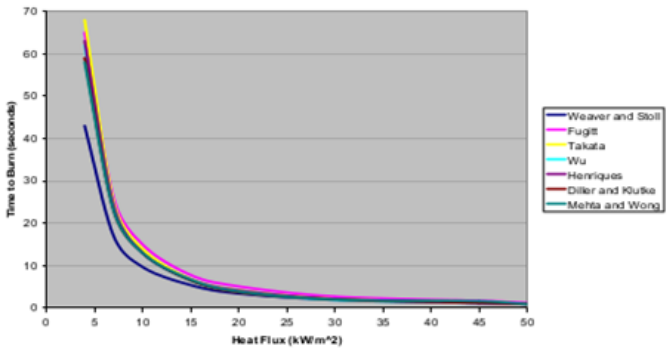


Fig. 4.5 First Degree Burn-Predicted Time

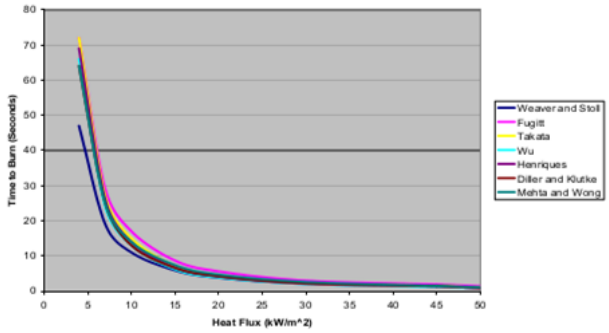


Fig 4.6 Superficial Second Degree Burn-Predicted Time

### 4.6 Stoll and Chianta Criterion

Stoll and Chianta created a straightforward technique for forecasting second-degree burns based on experimentally recorded times to onset. A succession of heat flow loads were recorded, and the corresponding temperature rise of a copper ball calorimeter—as defined by ASTM E 457-96 was plotted to create stall and Chianta curves. The intersection point shows the point of combustion when a temperature plotted across the Stall and Chianta curves is applied to a copper ball calorimeter subjected to a square wave heat flux. The data for constructing the curves are shown in Table 4.3.

| Time | Heat Flux to Cause 2nd Deg Burn | | Total Energy Absorbed | | Calorimeter Equivalent Temp Rise | |
|---|---|---|---|---|---|---|
| | cal/cm^2*s | kW/m^2 | cal/cm^2 | kJ/m^2 | Def F | Deg C |
| 1 | 1.2 | 50 | 1.20 | 50 | 16.0 | 8.9 |
| 2 | 0.73 | 31 | 1.46 | 61 | 19.5 | 10.8 |
| 3 | 0.55 | 23 | 1.65 | 69 | 22.0 | 12.2 |
| 4 | 0.45 | 19 | 1.80 | 75 | 24.0 | 13.3 |
| 5 | 0.38 | 16 | 1.90 | 80 | 25.3 | 14.1 |
| 6 | 0.34 | 14 | 2.04 | 85 | 27.2 | 15.1 |
| 7 | 0.30 | 13 | 2.10 | 88 | 28.0 | 15.5 |
| 8 | 0.274 | 11.5 | 2.19 | 92 | 29.2 | 16.2 |
| 9 | 0.252 | 10.6 | 2.27 | 95 | 30.2 | 16.8 |
| 10 | 0.233 | 9.8 | 2.33 | 98 | 31.1 | 17.3 |
| 11 | 0.219 | 9.2 | 2.41 | 101 | 32.1 | 17.8 |
| 12 | 0.205 | 8.6 | 2.46 | 103 | 32.8 | 18.2 |
| 13 | 0.194 | 8.1 | 2.52 | 106 | 33.6 | 18.7 |
| 14 | 0.184 | 7.7 | 2.58 | 108 | 34.3 | 19.1 |
| 15 | 0.177 | 7.4 | 2.66 | 111 | 35.4 | 19.7 |
| 16 | 0.168 | 7.0 | 2.69 | 113 | 35.8 | 19.8 |
| 17 | 0.160 | 6.7 | 2.72 | 114 | 36.3 | 20.2 |
| 18 | 0.154 | 6.4 | 2.77 | 116 | 37.0 | 20.6 |
| 19 | 0.148 | 6.2 | 2.81 | 118 | 37.5 | 20.8 |
| 20 | 0.143 | 6.0 | 2.86 | 120 | 38.1 | 21.2 |
| 25 | 0.122 | 5.1 | 3.05 | 128 | 40.7 | 22.6 |
| 30 | 0.107 | 4.5 | 3.21 | 134 | 42.8 | 23.8 |

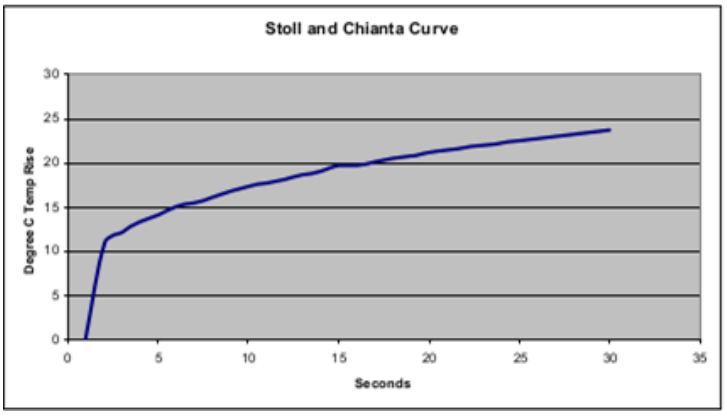


**Fig.4.7** Stoll and Chianta Curve

### 4.7 CFD Temperature and Heat Flux Plots

Fig 4.8 shows the temperature distribution on the vertical section cut taken along the burner axis and heat flux distribution on the manikin surface is shown in the right.

The temperature and heat flux plots are shown at various time instances of the flash flame event. The flame get stable 1 second after the initiation of ignition. The maximum heat flux is observed at the upper thigh resion of the manikin where the flame hits.

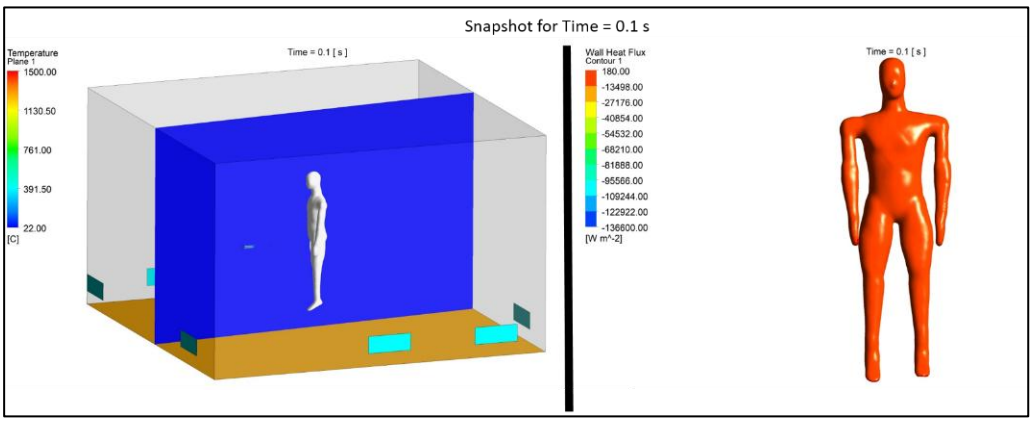


Time at 0.1 Sec

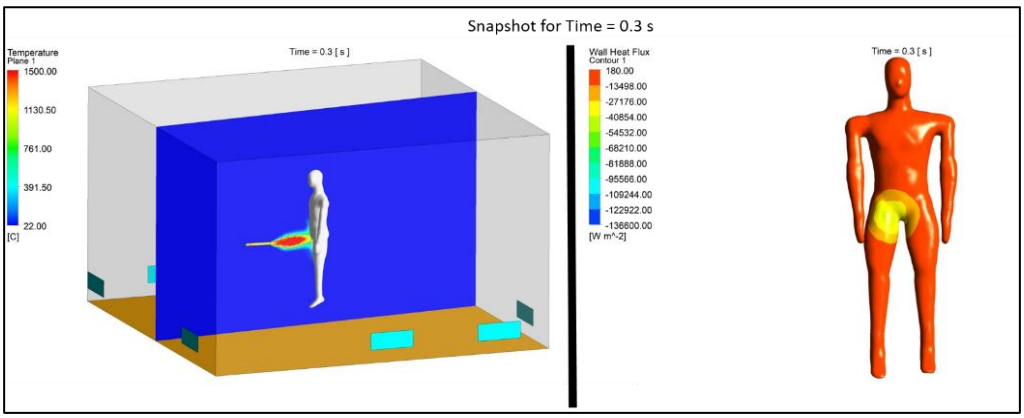


Time at 0.3 Sec

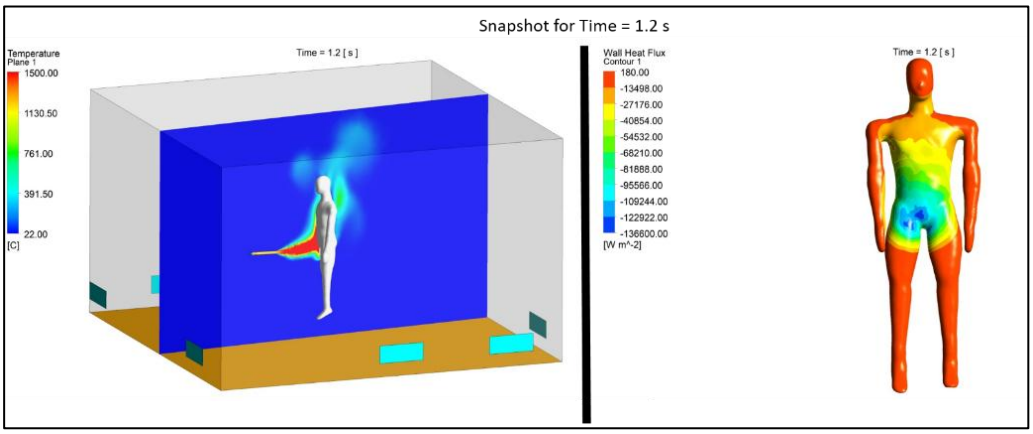


Time at 1.2 Sec

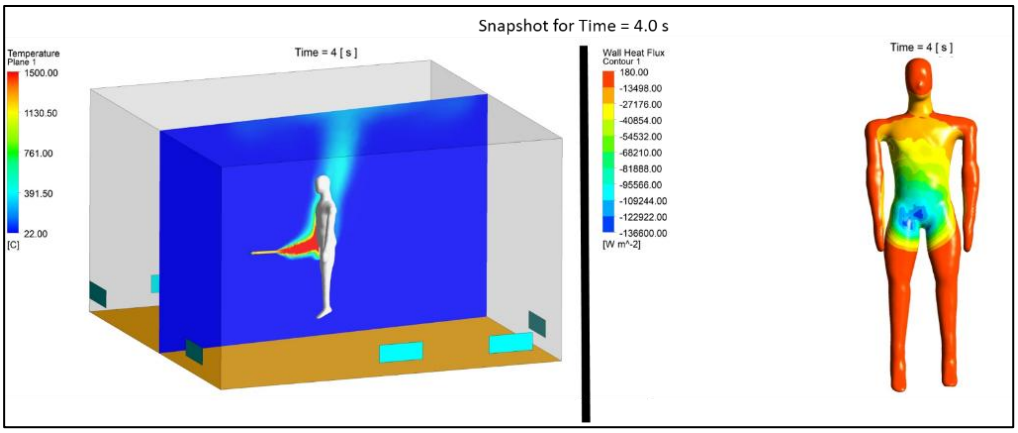


Time at 4.0 Sec

**Fig.4.8** heat flux distribution on the manikin at various time instances

# CHAPTER 5

## RESULTS & DISCUSSION

This chapter presents the obtained results. The system is described in detail with its specifications and assumptions. Parametric investigation is carried out to find out the impact of different input parameters on the outcomes.

In this study, a manikin with fire suit was exposed to a heat flux of 84 kW/m2 in this investigation, and the temperature increase that resulted was measured. The arrangement of the 12 burner groups is seen in Figure 3. Twelve industrial propane burners run on it (propane makes up 90% of the fuel, butane makes up 5%, and propylene makes up 5%). As illustrated in Fig. 4.3, the manikin is outfitted with 134 heat flux sensors spaced across its body. For every sensor position, a computer system manages data collection, computes surface heat flow and skin temperature distribution histories, and forecasts skin burn damage.

.

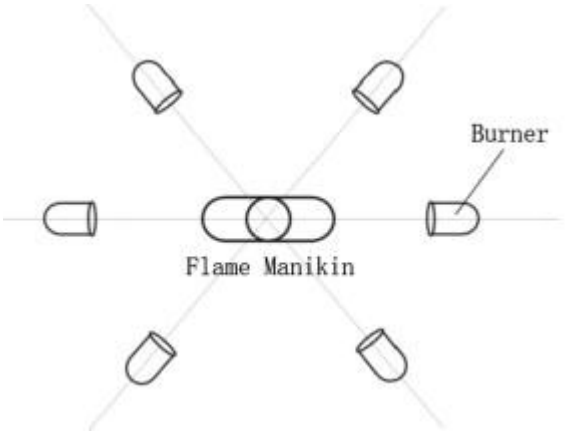


**Fig. 5.1** Layout of 12 burners in 2 groups

### 5.2 Temperature profile inside human skin during testing

Temperature over time for different heat flux for experimental data plotted.

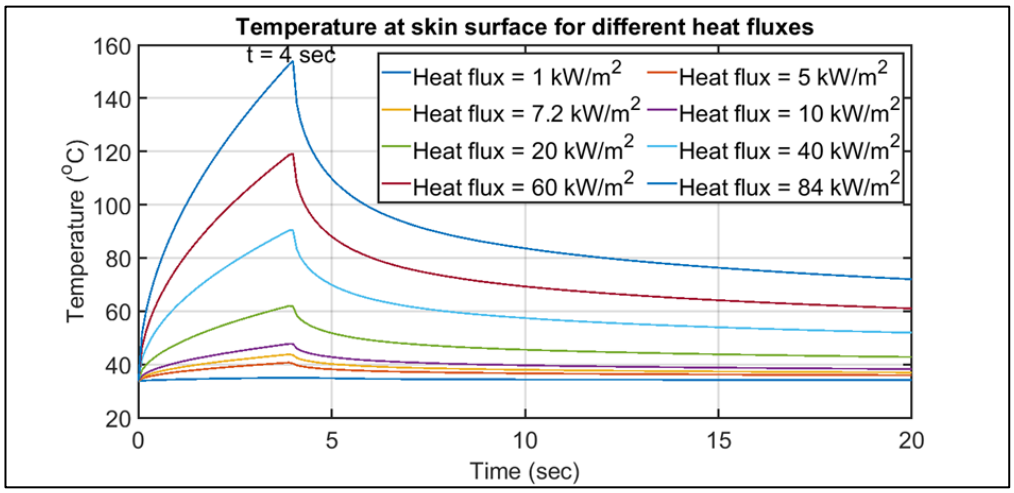


**Fig 5.2** Effect of changing heat flux on Skin surface

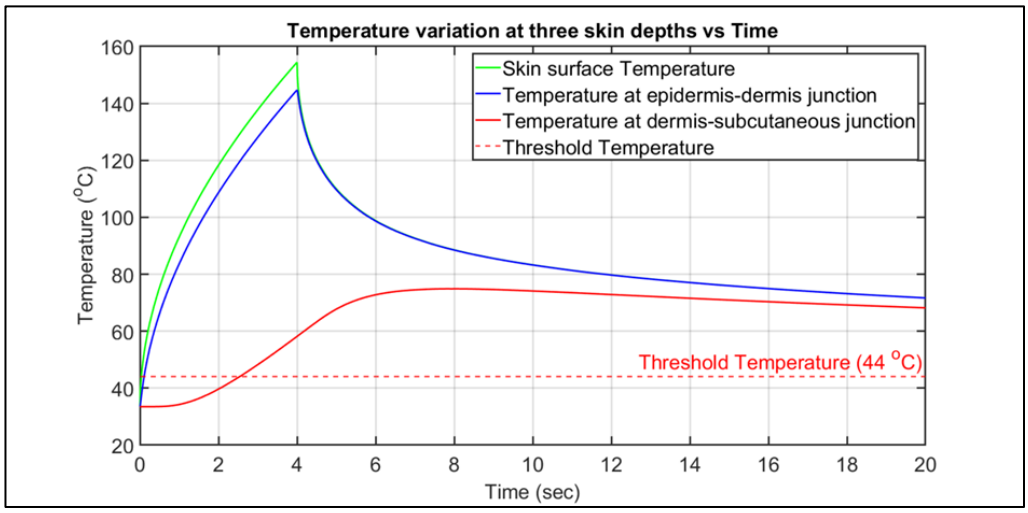


**Fig 5.3** Temperature variation at junctions of skin layers

### 5.3 comparison of CFD vs experimental manikin heat flux

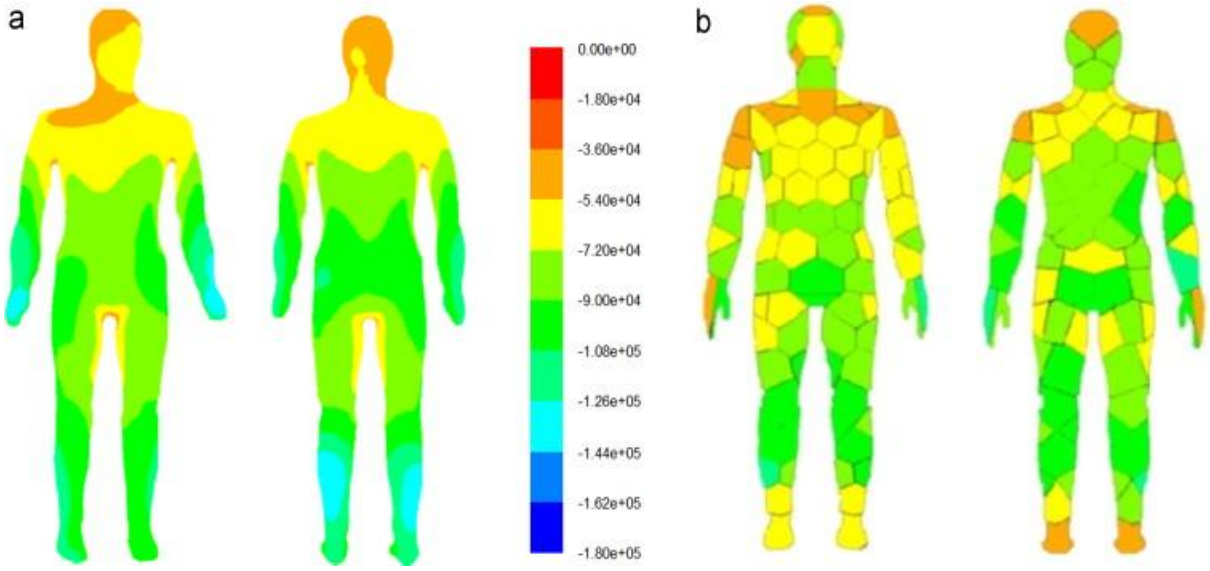


**Fig. 5.4** (a) Comparison of heat flux (KW/m$^2$) profiles on the surface of the CFD manikin and (b) Experimental manikin at the 4$^{th}$ second after flaming

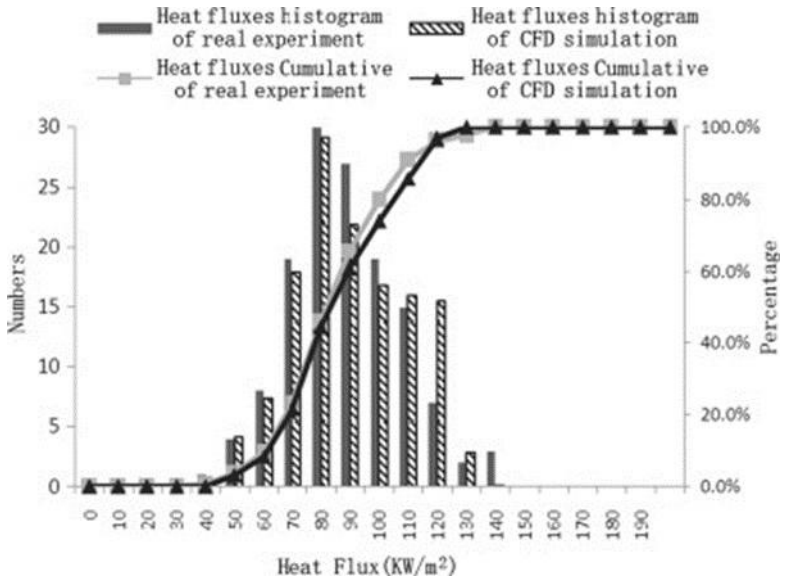


**Fig. 5.5** Comparisons of heat fluxes histogram of actual manikin tests and CFD simulation result

The results obtained show that the experimental model has good relationship with the CFD model and the results obtained with regards to heat flux, temperature variations are within the rage of 5%.

A numerical model developed for simulating real life behaviour of fire protective clothing (FPC). Fabric parameters like thickness, geometry etc. and other parameters like thermal and mechanical properties will be incorporated in modelling.

The numerical model analysed and the results compared with the actual experimental data available or the reported literature. An overlap of comparison between the experimental results and the simulation results validate the numerical model. If the required overlap is not achieved the numerical model should be accordingly modified to correctly predict the real behaviour.

The Manikin was subjected to artificially generated heat flux and the temperature variations at 134 points on the manikin were recorded.

The Manikin used for experimentation was drawn having same configurations as used for the experimentation. The geometry so produced was imported in the ANSYS Fluent. Meshing as well as boundary layer meshing was created on the imported geometry. The CFD modelling was modified according to the experimental inlet heat flux. The various properties were incorporated. This was done to take care of the distortions in the heat flow field.

In the pre study various models such as k- ε, k- ω, Reynolds stress model to verify the CFD model with the experimental results. It was found that the turbulence model of RNG, k- ε had shown better results and were in accordance with the experimental results.

Once model was finalized, Grid independence test was tested with different mesh sizes was carried out, but the results with 0.7 mm were found to be near to the experimental results.

CFD analysis was carried out to further determine the performance of heat flux at various time intervals

# CHAPTER 6

# CONCLUSIONS AND DIRECTIONS FOR FUTURE RESEARCH

This chapter summarizes the main findings of the study and indicates directions for future research work.

## 6.1 CONCLUSIONS

In this study, 3D CFD simulations were used to study heat and mass transfer in a fire test system for thermal protective clothing against the human body. The grid model used, simulated by the manikin, has real dimensions and an accurate shape of a typical man. The temperature and velocity fields across the chamber determined by the CFD simulations in the naked manikin test with a 4 second flash exposure show reasonable distributions. A real manikin test is also performed for further verification. By comparison, the simulated results of the heat flux distribution on the manikin surface are basically consistent with the actual experimental results. The heat flow in the main part of the body, the torso, is very close to the measured value. However, the heat flow in the limbs in the CFD simulation is higher than in the actual measurements. One of the main reasons for localized errors is the smaller size of the chamber in the simulation than in the real chamber. The heat flow accumulation curves in the CFD simulations are very close to the curves measured with 134 sensors in experiments with real manikin. Based on these results, we conclude that the CFD model can predict the temperature and velocity fields throughout the chamber in the manikin test.

Clothing used was also able resist the heat transfer within as per the internationally accepted ASTM F1930 standard.

Injury prediction was also predicted accurately with the present study

## 6.2 SUGGESTION/ DIRECTIONS FOR FUTURE RESEARCH

1. Experimental analysis to be carried out to obtain actual results in real environment.

## REFERENCES


1. Sipe, J.E., 2004. Development of an instrumented dynamic mannequin test to rate the protection provided by protective clothing. Development, 2004, pp.05-03.
2. National Fire Protection Association, 2007, NFPA 2112: standard on flame resistant garments for protection of industrial personnel against flash fire.
3. Morse, H.L., Thompson, J.G., Clark, K.J., Green, K.A. and Moyer, C.B., 1973. Analysis of the thermal response of protective fabrics. DTIC Document.
4. Heat and Mass Transfer in Multilayer Fabrics, S.Quiniou, *F.Lesage1,* V.Ventenat *and* M.A.Latifi, Laboratoire des Sciences du Génie Chimique, CNRS-ENSIC, B.P.20451, 1 rue Grandville, 54001, Nancy Cedex, France.
5. Yunyi Wang, Yijing Zong, 2011 "Evaluating the moisture transfer property of the multi-layered fabric system in fire-fighter turnout clothing", Fibres & Textiles in eastern Europe 2011, vol. 19, No.6(89) pp. 101-105.
6. James J Barry, Roger W Hill, 2003, "Computational Modeling of Protective Clothing", INJ Fall 2003, pp. 25-34.
7. Ahmed Ghazy, Donald J Bergstrom, 2012, "Numerical simulation of heat transfer in firefighters' protective clothing with multiple air gaps during flash fire exposure", An international journal of computation and methodology, 61:8, 569-593.
8. Yun Su, Yunyi Wang and Jun Li, "Evaluation method for thermal protection of firefighters clothing in high-temperature and high-humidity condition", International Journal of clothing Science and Technology, vol. 28 No.4, 2016, pp. 429-448.
9. Miao Tian, Zhaoli Wang, Jun Li, "3D numerical simulation of heat transfer through simplified protective clothing during fire exposure by CFD", International Journal of Heat and Mass Transfer, 93, 2016, 314-321.
10. S F Neves, J B L M Campos, T S Mayor, "On the determination of parameters required for numerical studies of heat and mass transfer through textiles – Methodologies and experimental procedures", International Journal of Heat and Mass Transfer, 81, 2015, 272-282.

11. Udayraj, Prabal Talukdar, R Alagirusamy, A Das, “Heat transfer analysis and second degree burn prediction in human skin exposed to flame and radiant heat using dual phase lag phenomenon”, International journal of heat and mass transfer, 78, 2014, 1068-1079.
12. Mobedi, M. and Gediz Ilis, G., 2023. One-Dimensional Unsteady Heat Conduction in a Cartesian Coordinate System. In Fundamentals of Heat Transfer: An Interdisciplinary Analytical Approach (pp. 37-50). Singapore: Springer Nature Singapore.
13. Launder, B.E. and Spalding, D.B., 1983. The numerical computation of turbulent flows. In Numerical prediction of flow, heat transfer, turbulence and combustion (pp. 96-116). Pergamon.
14. Dagur, R., Singh, V., Grover, S., Sethi, N. and Arora, B.B., 2018. Design of flying wing UAV and effect of winglets on its performance. International Journal Emerging Technology Advance Engineering, 8(3).
15. Arora, B.B. and Pathak, B.D., 2011. CFD analysis of axial annular diffuser with both hub and casing diverging at unequal angles. International Journal of Dynamics of Fluids, 7(1), pp.109-122.
16. ASTM F1930-18, Standard Test Method for Evaluation of Flame-Resistant Clothing for protection against fire simulations using instrumented Manikin.
17. Miao Tian, Yun Su and Jun Li, 2024. Simulating heat transfer from the fire environment to protective clothing and human body using CFD and predicting skin burn distribution. Journal of Tsinghua university (Science & Technology), 64(6), pp. 1032-1038.

# Publications from Current Work

Based on the present study, the following papers have been published.

**Journal Paper SCOPUS Published/Accepted**

1. Rai, A.K. and Arora, B.B., 2023. Analysis of Fire Suit with Flame Test Manikin System. *Journal of Advanced Zoology*, *44*(S6), pp.225-230. (Published)
2. Rai, A.K. and Arora, B.B., 2023. Different Testing Methods of Heat Resistant Fire Protective Fabric & Clothing. *Utilitas Mathematica, ISSN: 0315-3681* (Accepted)

**Journal Paper Published in International Journal**

1. Rai, A.K. and Arora, B.B., 2023. CFD Modelling of Flame Test Mannequin System. *International Journal of Advanced Research and Innovation, ISSN: 2347-3258* (Published)

# AUTHOR'S BIODATA

Ashutosh Kumar Rai has pursued his Graduation (B.E.) in Mechanical Engineering from Jamia Millia Islamia in the year 2010 and Post-Graduation (M.Tech.) in Thermal Engineering from Delhi Technological University in the year 2013.

He has 23 years of working experience in the field of Mechanical Engineering. His area of experience is Operation and Maintenance of Thermal Power Plant, Bio-fuels, renewable energy and Fire Suit testing including firefighting training.

He has published 7 numbers of research papers in different international journals.